Report No. IITRI-U6002-47
(Triannual Report)

DEVELOPMENT OF SPACE-STABLE THERMAL-CONTROL COATINGS

George C. Marshall Space Flight Center
National Aeronautics & Space Administration

IIT RESEARCH INSTITUTE

Report No. IITRI-U6002-47
(Triannual Report)

DEVELOPMENT OF SPACE-STABLE THERMAL-CONTROL COATINGS

Contract No. NAS8-5379
IITRI Project U6002

Funded Under Code

124-09-05-26-62

Prepared by

G. A. Zerlaut
F. O. Rogers

Submitted by

IIT RESEARCH INSTITUTE
Technology Center
Chicago, Illinois 60616

to

George C. Marshall Space Flight Center
National Aeronautics & Space Administration
Huntsville, Alabama

Copy No. ____

November 30, 1966

FOREWORD

This is Report No. IITRI-U6002-47 (Triannual Report) of IITRI Project U6002, Contract No. NAS8-5379, entitled "Investigation of Environmental Effects on Coatings for Thermal Control of Large Space Vehicles." This report covers the period from June 20 through October 20, 1966. Previous Triannual Reports were issued on October 25, 1963; March 5, 1964, July 20, 1964; December 21, 1964; February 23, 1965; July 20, 1965; November 9, 1965; February 21, 1966 and July 11, 1966.

Major contributors to the program during this period include Gene A. Zerlaut, project leader and, alphabetically; Noel D. Bennett, reflectance measurements and space-simulation tests; William C. Courtney, consultation on vacuum problems; Wayne Ridenour, vacuum equipment design; Frederick O. Rogers, zinc titanate synthesis and paint formulations; Dr. Robert G. Scholz, mass spectrometry studies; Raymond Serway, electron spin resonance studies; and Samuel Shelfo, reflectance measurements and space simulation tests. Dr. T. H. Meltzer, Manager of Polymer Research, provided administrative supervision. The work reported herein was performed under the technical direction of the Research Projects Laboratory of the George C. Marshall Space Flight Center with Daniel W. Gates acting as Project Manager.

Contributions to this report were prepared by F. O. Rogers, R. A. Serway and Dr. R. G. Scholz.

Prior to March 15, 1966, this contract was funded under Codes 993-50-01-00-00, 124-09-05-00-14, and 908-20-02-01-47.

Respectfully submitted,
IIT RESEARCH INSTITUTE

Approved by:

T. H. Meltzer
Manager
Polymer Research

G. A. Zerlaut
Group Leader
Polymer Research

GAZ/am

IIT RESEARCH INSTITUTE

ABSTRACT

The work reported consists of (1) space-simulation tests on inorganic powders and coatings employing both post-exposure and in situ-reflectance measurements, (2) synthesis of zinc titanate pigment, (3) evaluation of the optical and stability characteristics of zinc titanate and zinc titanate-pigmented coatings, (4) solvent studies pertaining to various silicone paints, (5) methyl silicone photolysis studies, and (6) check-out and calibration tests on the new In Situ Reflectometer/ Irradiation Facility (IRIF).

TABLE OF CONTENTS

		Page
Abstract		iii
I.	Introduction	2
II.	Inorganic Technology	2
	A. Simulation Tests Employing Post-Exposure Measurements	2
	B. Simulation Tests Employing In Situ Measurements	4
	C. Zinc Titanate Pigment Investigations	7
III.	Methyl Silicone Paints	35
	A. Simulation Tests Employing Post-Exposure Measurements	35
	B. Solubility Studies of Silicone Resins	35
IV.	Silicone Photolysis Studies	42
	A. Introduction	42
	B. Irradiation Procedure and Analysis of Mass Spectra	43
	C. Analysis of ESR Spectra	50
V.	The IRIF	56
VI.	Summary of Results	73
Appendix		75
References		76

LIST OF TABLES

Table		Page
1	Results of 2000 ESH Simulated Solar UV on Several Inorganic Specimens	3
2	Results of 500 ESH in Situ Space Simulation on Several Inorganic Powder Specimens	5
3	Optical Density-Reflectance Conversions (R_λ = 80%)	4
4	Synthesis Schedule of Several Zinc Orthotitanates	20
5	Synthesis Schedule of Several Different Zinc Titanates of Stoichiometry	25
6	Effect of 1000-ESH UV on the Reflectance of Several Pigment Powders	33
7	Results of 2000 ESH Simulation Test on Several Zinc Titanate-Pigmented Silicone Paints	36
8	Solubility of RTV-602 in Various Solvents	38 39
9	Solubility of Owens-Illinois Glass Resin 901	41

LIST OF FIGURES

Figure		Page
1	Spectral Reflectance of New Jersey Zinc's A-54-2 Zinc Titanate (Wet-Sprayed Powder)	13
2	Spectral Reflectance of TAM's "B" and CP Zinc Titanate (Wet-Sprayed Powders)	14
3	Spectral Reflectance of Precursor Oxides to Zinc Titanate: Zinc Oxide, Rutile and Anatase (Wet-Sprayed Powders)	15
4	Spectral Reflectance of IITRI Batch A-104 Zinc Titanate (Wet-Sprayed Powder)	16
5	Spectral Reflectance of Forsterite (Merck) and Zinc Magnesium Titanate (TAM) (Wet-Sprayed Powders)	17
6	Spectral Reflectance of IITRI Batch A-104-A Zinc Titanate (Wet-Sprayed Powders)	19
7	Spectral Reflectance of IITRI Batch A-111 Zinc Titanate (Wet-Sprayed Powder)	21
8	Spectral Reflectance of IITRI Batch A-111-A Zinc Titanate Prepared from Batch A-111 (Wet-Sprayed Powder)	22
9	Spectral Reflectance of IITRI Batch A-114 Zinc Titanate (Wet-Sprayed Powder)	23
10	Spectral Reflectance of IITRI Batch A-115 Zinc Titanate (Wet-Sprayed Powder)	24
11	Spectral Reflectance of IITRI Batch A-129 Zinc Titanate (Wet-Sprayed Powder)	26
12	Spectral Reflectance of IITRI Batch A-130 Zinc Titanate (Wet-Sprayed Powder)	28
13	Spectral Reflectance of IITRI Batch A-131 Zinc Titanate (Wet-Sprayed Powder)	29
14	Spectral Reflectance of IITRI Batch A-132 Zinc Titanate (Wet-Sprayed Powder)	30

LIST OF FIGURES (CONT.)

Figure		Page
15	Spectral Reflectance of IITRI Batch A-133 Zinc Titanate (Wet-Sprayed Powder)	31
16	Schematic (Side View) of the Photolysis Train	44
17	Schematic (End View) of the Photolysis Train	45
18	Schematic (Top View) of the Photolysis Train	46
19	The Hitachi RMU-6D Mass Spectrometer	47
20	The Electron-Spin-Resonance Spectrometer	48
21	Electron-Spin-Resonance-Absorption Spectrum of LP-5 Polydimethylsiloxane Irradiated with UV at 77°K	51
22	Electron-Spin-Resonance-Absorption Spectrum of LP-5 Polydimethylsiloxane Irradiated with UV at 77°K (Same as Figure 21 with Gain Times 5)	52
23	Schematic of UV-Irradiated Facility with in Situ Reflectance Capability (The IRIF)	57
24	Section of IRIF's Engineering Assembly Drawing Showing Integrating Sphere and UV-Irradiation Chamber	58
25	Schematic of the Sample Table Assembly and Interchange Mechanism	60
26	Section of IRIF's Engineering Assembly Drawing Showing UV-Irradiation Chamber and Manipulators (Top View)	61
27	Section of IRIF's Engineering Assembly Drawing Showing the UV-Irradiation Chamber (Top View)	62
28	Section of IRIF's Engineering Assembly Drawing Showing Manipulators, Rach and Pinion, and Magnetic Chuck	63

LIST OF FIGURES (CONT.)

Figure		Page
29	The IRIF Mated to the Beckman DK-2A Spectroreflectometer	65
30	The IRIF's 400 Liter/Sec Vac-Ion Pump and Heavy-Duty Dolly	66
31	Top View of the IRIF's UV-Irradiation Chamber Showing Samples, Sample Table and Manipulator Arms	67
32	IRIF's Integrating-Sphere Hemisphere Showing Empty Sample Holder and Shutter	68
33	IRIF's Removable Hemishere Showing Spherical Segment with Photomultiplier Tube and Lead Sulfide Cell Attached	69

DEVELOPMENT OF SPACE-STABLE THERMAL-CONTROL COATINGS

I. INTRODUCTION

The general requirement under this contract is for the development of thermal-control surface coatings which possess very low but stable ratios of solar absorptance (α_s) to infrared emittance (ε_H). The program has been divided historically into three major phases; (1) inorganic technology, (2) silicone photolysis and silicone paint investigations, and (3) general coatings investigations.

The relative emphasis placed upon each of these three major tasks has varied during the course of the program in accordance with the urgency of the various problems elucidated by our investigations, as well as the availability of both funds and personnel.

The work reported herein consists of (1) space-simulation tests on inorganic powders and coatings employing both post-exposure and in situ reflectance measurements, (2) synthesis of zinc titanate pigment, (3) evaluation of the optical and stability characteristics of zinc titanate and zinc titanate-pigmented coatings, (4) solvent studies pertaining to various silicone paints, (5) methyl silicone photolysis studies, and (6) check-out and calibration tests on the new In Situ Reflectometer Irradiation Facility (IRIF).

II. INORGANIC TECHNOLOGY

A. Simulation Tests Employing Post-Exposure Measurements

Table 1 is a presentation of the results of two space simulation tests Q-20 and Q-21, on inorganic specimens. These tests employed post-exposure-reflectance measurements obtained with the Beckman DK-2A spectroreflectometer; the data were obtained by comparison to freshly smoked magnesium oxide.

Specimens 5268 through 5270 are samples obtained by the NASA program manager from NASA's Goddard Space Flight Center. The $\Delta\alpha$ of 5268, an Al_2O_3-pigmented potassium silicate paint, was more than twice as great as the value exhibited by a specimen (5218) of the same coating irradiated in an earlier test (see Table 4, Triannual Report IITRI-U6002-42). The stabilities exhibited by CM-118 and CM-119 in Test Q-20 are more nearly comparable to those exhibited in the earlier test. The $\Delta\alpha$'s of CM-114, CM-118 and CM-119 were 0.073, 0.035 and 0.058, respectively, in the earlier 1650-ESH test. (It should be noted that Table 4 in Triannual Report IITRI-U6002-42 has been found to be in error insofar as CM-118 is the rutile paint and CM-119 is the zinc oxide paint as determined by the notations supplied by NASA).

The three "wet sprayed" powder specimens 5275, 5276, and 5277 underwent degradation in Test Q-21 (Table 1) which helps to interpret the data obtained on these three specimens when irradiated in Test I-4 (see Table 2). None of the three were observed to undergo "bleachable" infrared degradation in Test I-4. However, the method of data analysis consisted of normalizing the in situ optical density curves at 700 mμ, which belied the extent of damage that occurred in the visible portion of the spectrum. Thus, the greying which was observed visually in Test I-4 has subsequently been determined, on the basis of Test Q-21, to be slight for the "protected" rutile samples and great for the titanium pyrophosphate specimen. The protected rutile did not possess high reflectance in the solar spectrum, however.

Table 1

RESULTS OF 2000 ESH SIMULATED SOLAR UV
ON SEVERAL INORGANIC SPECIMENS

Specimen No.	Material	Test	Exposure[1] (ESH)	Solar Absorptance α_1	α_2	α_3	$\Delta\alpha$
5268	CM114[2]	Q-20	0	.101	.140	.241	-
	Al_2O_3/KSil		2000	.269	.140	.409	.168
5269	CM118[2]	Q-20	0	.097	.110	.207	-
	TiO_2/KSil		2000	.134	.106	.240	.033
5270	CM119[2]	Q-20	0	.117	.116	.233	-
	ZnO/KSil		2000	.165	.109	.274	.041
5275	TiP_2O_7[3]	Q-21	0	.095	.089	.184	-
			2000	.180	.109	.289	.105
5276	TTP7T[3,4]	Q-21	0	.185	.178	.363	-
			2000	.194	.183	.377	.014
5277	TTP97[3,4]	Q-21	0	.171	.168	.339	-
			2000	.194	.170	.364	.025
5278	Alumina[5]	Q-21	0	.112	.122	.234	-
			2000	.174	.124	.298	.064

[1] 2000 ESH at ~ 7 solar intensities

[2] Furnished by C.O.T.R. (NASA-Goddard Specimens)

[3] Powder specimen (wet sprayed)

[4] "Protected" rutile from Lexington Laboratories

[5] Flame-deposited alumina from "Telstar"

It should be noted that "wet spraying" consists of spraying a water mull of the pigment in question onto a warm, or hot, aluminum substrate. The coatings can be applied in thicknesses to several mills and if applied properly do not crack or spall when the water is driven off by heating at 200° F. The powder coatings offer an excellent method of evaluating close-packed, non-pressed, pigment candidates.

B. Simulation Tests Employing In Situ Measurements

The results of space simulation tests I-4, I-5, and I-6 are presented in Table 2. These tests all employed the *in situ* measurement of spectral reflectance using the apparatus described in the last two Triannual Reports (IITRI-U6002-36 and IITRI-U6002-42). Except for specimen 5257, all specimens discussed in Table 2 were wet-sprayed powders on aluminum substrates. The initial reflectance values could not be obtained without damaging the powders. The reflectance changes which the optical density changes shown in Table 2 represent are presented in Table 3 for the arbitrarily selected initial reflectance of 80%.

Table 3

OPTICAL DENSITY-REFLECTANCE CONVERSIONS
(R_λ = 80%)

ΔO.D.	ΔR_λ
.028	-5%
.035	-6%
.040	-7%
-.005	+1%
-.010	+2%
-.050	+10%
-.070	+14%
-.100	+20%

Table 2

RESULTS OF 500 ESH IN SITU SPACE SIMULATION ON SEVERAL INORGANIC POWDER SPECIMENS

Sample No.	Material	Test	ΔO.D. (Reflectance) 0.4μ	0.7μ	1.0μ	2.0μ
5254	TTP97[1]	I-4	.028	.000	.000	.000
5255	TTP7T[1]	I-4	.040	.000	.000	-.010
5256	TiP_2O_7	I-4	.035	.000	-.070	-.100
5257	Zn_2TiO_4/901	I-4	.000	.000	-.005	-.050
5258	r-TiO_2[2]	I-5	.025	.015	.015	.000
5259	$CaZrSiO_5$	I-5	.032	.000	.000	-.005
5260	$ZnZrSiO_5$	I-5	.030	.000	.000	.000
5261	SP500 ZnO[3]	I-5	.010	.000	.000	.050[4]
5262	SP500 ZnO	I-6	.005	.000	.000	.045
5263	PS7/ZnO	I-6	.025	.000	.000	.000
5264	r-TiO_2[2]	I-6	.028	.018	.008	-.010
5265	PS7/ZnO[5]	I-6	.013	.000	.000	.005

[1] Furnished by Lexington Laboratories, Inc. under NAS8-20162

[2] Cabot rutile

[3] Heat Treated at 650°C for 16 hr.

[4] ΔO.D. = .09 at 2.7

[5] Heat-treated at 700°C for 5 hr.

Specimens 5254 and 5255 are silicate-protected rutiles prepared by Lexington Laboratories, Inc.,* of Cambridge, Mass. As mentioned in the previous section (II.A.), the optical density increases for specimens 5254, 5255 and 5256 do not account for the greying which all three materials exhibited. The normalization of the spectral curves at 7000 A assumed that no damage occurred at that wavelength. Specimens which grey usually exhibit a reflectance decrease at 7000 A which would be normalized out in the data reduction methods employed. The bleaching exhibited by TiP_2O_7 (5256) in the infrared cannot be explained at this time. It could, however, be associated with loss of water and this may also be inferred from the results of another (single-sample) test of TiP_2O_7 which was difficult to pump down.

The Zn_2TiO_4-pigmented Owens-Illinois 901 resin paint did not noticeably degrade except at wavelengths below 3750 A. The 901 resin contains a siloxane plasticizer and considerable outgassing was noted on this and subsequent tests employing 901 resin. The reflectance increase in the infrared cannot be explained at this time, however. Further work with the 901 resin was terminated because of the outgassing problem exhibited by the cured material (even though excellent coating properties were obtained with the formulation used to prepare specimen 5257). Additional studies of the 901 resin are discussed in Section III.

The data presented in Table 2 also show that Cabot's "Flame-Process" rutile titanium dioxide, specimens 5258 and 5264, does not exhibit bleachable degradation in the infrared as does zinc oxide. We did obtain, however, optical density increases in the wavelength range 700 to 1000 mμ which were not normalized out in the data-reduction technique employed. It is not known if this degradation is bleachable since we were looking for degradation in the 2000 to 2700 mμ region and did not make post-exposure measurements in air.

---

*Contract NAS8-20162, NASA-Marshall Space Flight Center

The double zirconium silicates of calcium and zinc, specimens 5259 and 5260, were also stable in the infrared region. The infrared-reflectance loss exhibited by the two SP500 zinc oxide specimens, 5261 and 5262, was less than zinc oxide has exhibited in previous tests. Specimen 5261 was heat-treated for 16 hrs at 650°C.

Of special interest are the results of irradiation of two silicate-treated SP500 zinc oxide specimens, 5263 and 5265, in Test I-6. Specimen 5263 showed no "bleachable" infrared degradation. Specimen 5265, on the other hand, was heat-treated for 5 hr at 700°C and therefore required breaking up of the aggregates prior to the preparation of the water mull used for wet-spraying the powder samples. This specimen exhibited a slight bleachable infrared degradation of about 1% at 2.0 μ wavelength. As a result of this data and that obtained on another program, it has been postulated that the "breaking-up" of aggregates formed during the heat-treatment of the silicate-treated powder results in the creation of new, unprotected zinc oxide surfaces. Such fresh surfaces would most certainly behave like the unprotected zinc oxide powder and can be expected to absorb infrared in similar fashion. The rate of spectral absorptance increase would therefore depend upon the fraction of new surface exposed. The studies pertaining to the silicate treatment of zinc oxide are now being funded under Contract 951737, Subcontract NAS7-100, from the Jet Propulsion Laboratory. The IITRI project number is U6053.

C. Zinc Titanate Pigment Investigations

1. Introduction

The results of investigations of a commercial zinc titanate pigment were presented in the last Triannual Report (IITRI-U6002-42). The only zinc titanate to have both high reflectance and good stability to ultraviolet irradiation in vacuum was found to be New Jersey Zinc Company's A-54-2, which was chemically designated

as Zn_2TiO_4, the orthotitanate. The results of 2000-ESH space simulation tests on several methyl silicone paints pigmented with this material are discussed in section III. A.

An attempt to obtain larger working samples of A-54-2 was unsuccessful and it became necessary to prepare zinc titanate in our own laboratories. The ensuing paragraphs present a discussion of our studies of zinc titanate pigments of measured composition from which we hope to formulate coatings of improved performance.

2. Literature Search

A search of the literature on "zinc titanate" revealed at the onset some very interesting conflicts between various research papers on the subject. Careful work has been performed by some laboratories but at the time we commenced work in our own laboratories, complete agreement existed among all sources only on one zinc titanate, the orthotitanate (Zn_2TiO_4). The orthotitanate is a spinel which is formed from 2 moles of ZnO and 1 mol of TiO_2.

The literature on the subject of zinc titanate begins in France in 1888 with a report by M. Lucien Levy (ref. 1) on highly colored zinc titanates; the color was due probably to iron impurities in the "acid titanique". Levy's second paper (ref. 2) was published in 1889 and was entitled "Sur Quatre Nouveaux Titanates de Zinc"; it describes black crystals of "titanate dibasique" ($TiO_2 \cdot 2ZnO$), a "jaune masse" of "titanate sesquibasique" ($2TiO_2 \cdot 3ZnO$) and a "violette masse" of "titanate neutre" ($TiO_2 \cdot ZnO$). Other titanates mentioned by Levy (ref. 1,2,3) are the orthodititanate $Zn_3Ti_2O_7$, mesopentatitanate $Zn_4Ti_5O_{14}$ and paratitanate $ZnTi_3O_7$.

With the passage of years titanium dioxide became a highly important commercial white pigment and references to the highly colored titanates disappeared except when deliberately created with Fe, Co, Ni, Cr, Mn, etc., introduced into the spinel structure (ref. 4). In 1930, Taylor (ref. 5), an assistant professor at the University of Minnesota, but nevertheless publishing in Germany,

found only the orthotitanate $2ZnO \cdot TiO_2$ which he made from 2 moles of zinc oxide and 1 mole of TiO_2 heated at 1050°C for 24 hours. He reported the crystal pattern identical "mit dem Film eines naturalichen Spinells von Ceylon."

Since, in 1930, the only commercially produced titanium dioxide was anatase, it appears to be the crystalline form used by Taylor and other workers in the field during the 1930's. In 1937 Cole and Nelson (ref. 6) of the National Lead Company noted that while earlier literature claimed the existence of a metatitanate $ZnTiO_3$, no experimental data had been offered in substantiation. They then proceeded to investigate compositions in the range 67/33 to 41/59 percentage ZnO-to-TiO_2. Once again the anatase form must have been employed since they reported titanium dioxide as having been prepared from "ilmenite solution"; they showed diffraction lines of TiO_2 only as anatase and reported the initial reaction temperature between zinc oxide and titanium dioxide to be 430°C. The conclusions of Cole and Nelson (ref. 6) in general supported Taylor (ref. 5) insofar as they reported only one zinc titanate, Zn_2TiO_4; however, they added much data to substantiate the existance of solid solutions of TiO_2 in the orthotitanate with a corresponding change in size of the unit cell.

In 1960, Dulin and Rase (ref. 8) of the State University of New York's College of Ceramics published a study of "Phase Equilibria in the System ZnO-TiO_2." They confirmed the existence and structure of the orthotitanate but also reported the definite existence of metatitanate as a compound ($ZnTiO_3$) having the hexagonal structure of ilmenite and stable up to a temperature of 925°C. They did not detect any evidence of the solid solution listed by Cole and Nelson. They employed both anatase and rutile titanium dioxide.

In 1961 Bartram and Slepetys (ref. 9) published a paper which to some extent cleared up the discrepancies in previous studies. They listed the orthotitanate as most easily prepared

from sulfate type anatase and zinc oxide; a reaction time of 3 hours at 800° to 1000°C is required. The metatitanate, they found, required chloride process rutile and an optimum temperature of 850°C. The solid solution phenomenon claimed by earlier writers appeared to be explained by the claim of Bartram and Slepetys to a third zinc titanate ($Zn_2Ti_3O_8$). This is a defect spinel structure made from anatase and zinc oxide in ratios of 2 moles ZnO to 3 moles TiO_2 reacted at a temperature of 700°C for at least 100 hours.

In 1962, B.A. Loshkarev and associates in three papers (ref. 7,10,11) found only orthotitanate as a compound using only rutile and zinc oxide and temperatures up to 1400°C. The reaction between rutile and zinc oxide did not begin below 740°C. This may be compared with Cole and Nelson's findings of a reaction starting point of 430°C when anatase was used.

The continued existence of unreacted zinc oxide in the final product, regardless of composition, temperature or time, is confirmed by the Russian papers. They report "very intense shrinkage" (from 15 to 18%) in forming the orthotitanate at temperatures above 1000°C. They therefore recommended slow heating when reaching this range. (We followed this advice in our samples A-132 and A-133 described in the next section; the high shrinkage was quite apparent). The Russian papers do not concede the existence of the metatitanate, $ZnO \cdot TiO_2$, nor the sesquititanate listed by Bartram and Slepetys.

The most recent publication on the subject is a Japanese paper by Kubo et al (ref. 12) which appears on cursory examination to be the most complete to date. We have only very recently obtained its translation and have been unable to make full use of it thus far. However, they acknowledge the existence of the three titanates and succeeded in making the metatitanate of exceptional purity.

Summarizing the literature, all workers agreed on the orthotitanate as to composition, crystal structure and characteristics. A few agreed upon the existence and structure of the metatitanate, and one only claimed the existence and structure of the defect spinel, $Zn_2Ti_3O_8$, which we will refer to in the future as the sesquititanate. It was considered best therefore to first attempt to form an orthotitanate using the method of Bartram and Slepetys slightly modified to fit our own equipment.

3. Experimental Procedures

Six batches of zinc titanate have been prepared and evaluated to date. Although the pertinent composition and reaction information are summarized in Table 5, the complete synthetic and evaluation procedures are discussed for batch A-104 in the following remarks.

Sample A-104

(A)	TiO_2 (TiPure FF anatase)	80 gms
	H_2O (Distilled)	320 gms
	NH_4OH (to pH of 8 or 9)	2 drps
(B)	ZnO (SP 500)	160 gms
	H_2O (Distilled)	285 gms

(C) A and B are each slurried for 5 min, combined and slurried together for 15 min.

(D) The slurry (C) is vacuum filtered to a cake using a Büchner funnel.

(E) The cake (D) is removed, spread on an aluminum sheet and dried at 100°C for 3 hours in a forced-air oven.

(F) The material (E) is broken up to a fine powder with a glass muller, packed into a porcelain crucible, and fired at 800°C for 3 hours.

The result of the above process was a very white pigment, brighter to the eye than any of the zinc titanate samples obtained from outside sources and present in sufficient quantity to permit the laboratory formulation of thermal-control coatings. The pigment also appeared whiter than either of the pigments from which it was made.

The absolute hemispherical spectral reflectance of pigment A-104 and several other pigment candidates were determined on our Edwards-type integrating-sphere attachment for the Beckman DK-2A spectrophotometer. Figures 1 and 2 show the near-ultraviolet and visible reflectance spectra of "wet sprayed" powder specimens of New Jersey Zinc Company's A-54-2 and Titanium Alloy Manufacturing's (TAM) "B" and "CP" zinc titanates, respectively. (All reflectance spectra discussed in this section were obtained on "wet sprayed" powder specimens prepared according to the procedures discussed in a previous section). Figure 3 is a presentation of the reflectance spectra of zinc oxide, rutile and anatase -- the ingredients from which zinc titanate is prepared. Figure 4 shows the reflectance spectra of IITRI's batch A-104 zinc titanate both as prepared and extracted with acetic acid. Figure 5 contains the spectra of two materials which are also of interest; Merck's forsterite, or magnesium silicate, and TAM's zinc magnesium titanate.

The reflectance curve for batch A-104 (Figure 4) showed unmistakably the formation of a compound with a reflectance in the near ultraviolet and short end of the visible spectrum totally unlike any other white pigment previously tested except for early batches of New Jersey Zinc's A-54-2 (not shown) which also showed the "step" in the reflectance spectra at about 3500-A wavelength. The latest and final batch of A-54-2 (Figure 1) does not show the severe step exhibited by previous batches and by the pigment obtained from TAM (Figure 2).

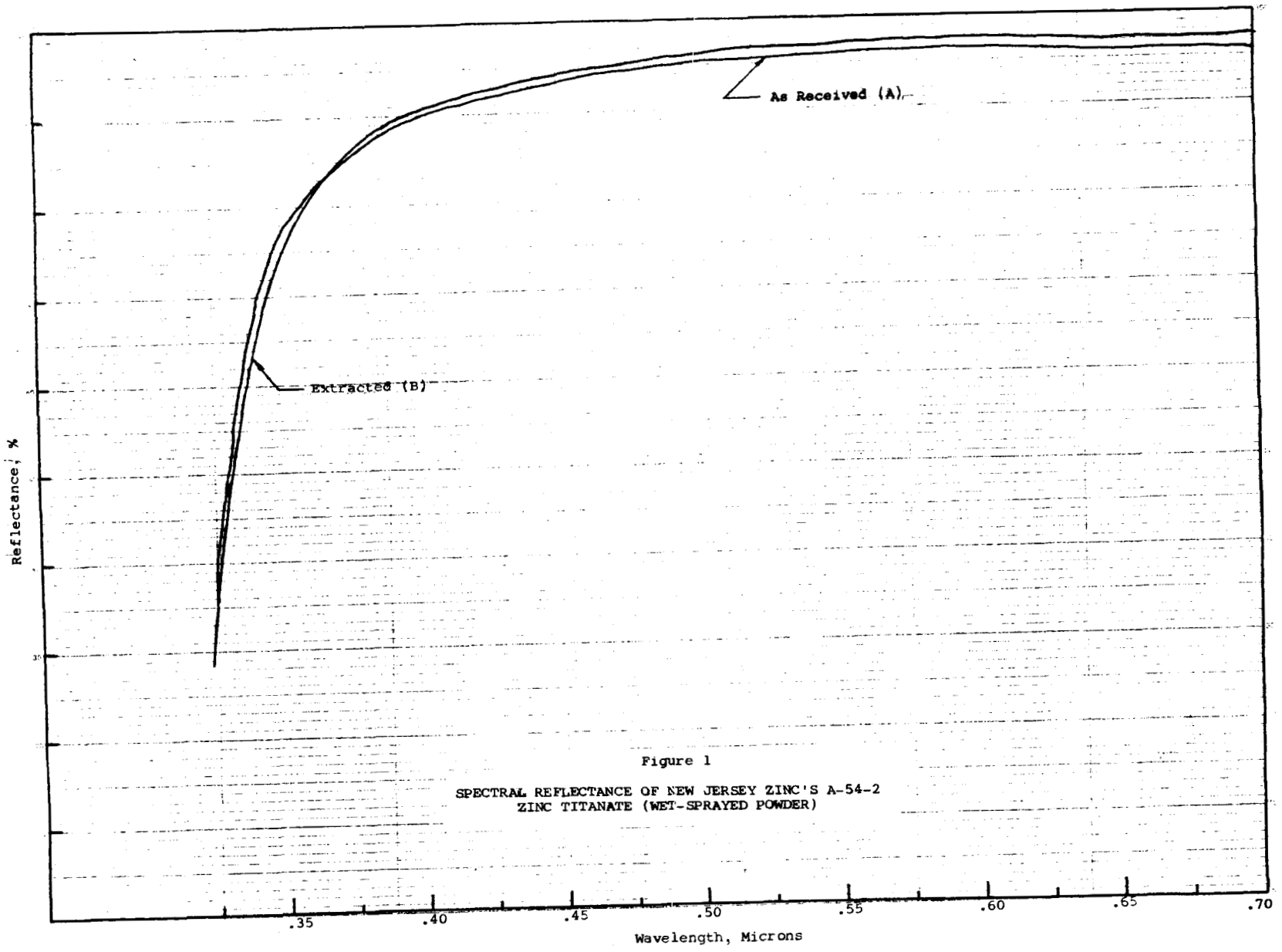

Figure 1

SPECTRAL REFLECTANCE OF NEW JERSEY ZINC'S A-54-2
ZINC TITANATE (WET-SPRAYED POWDER)

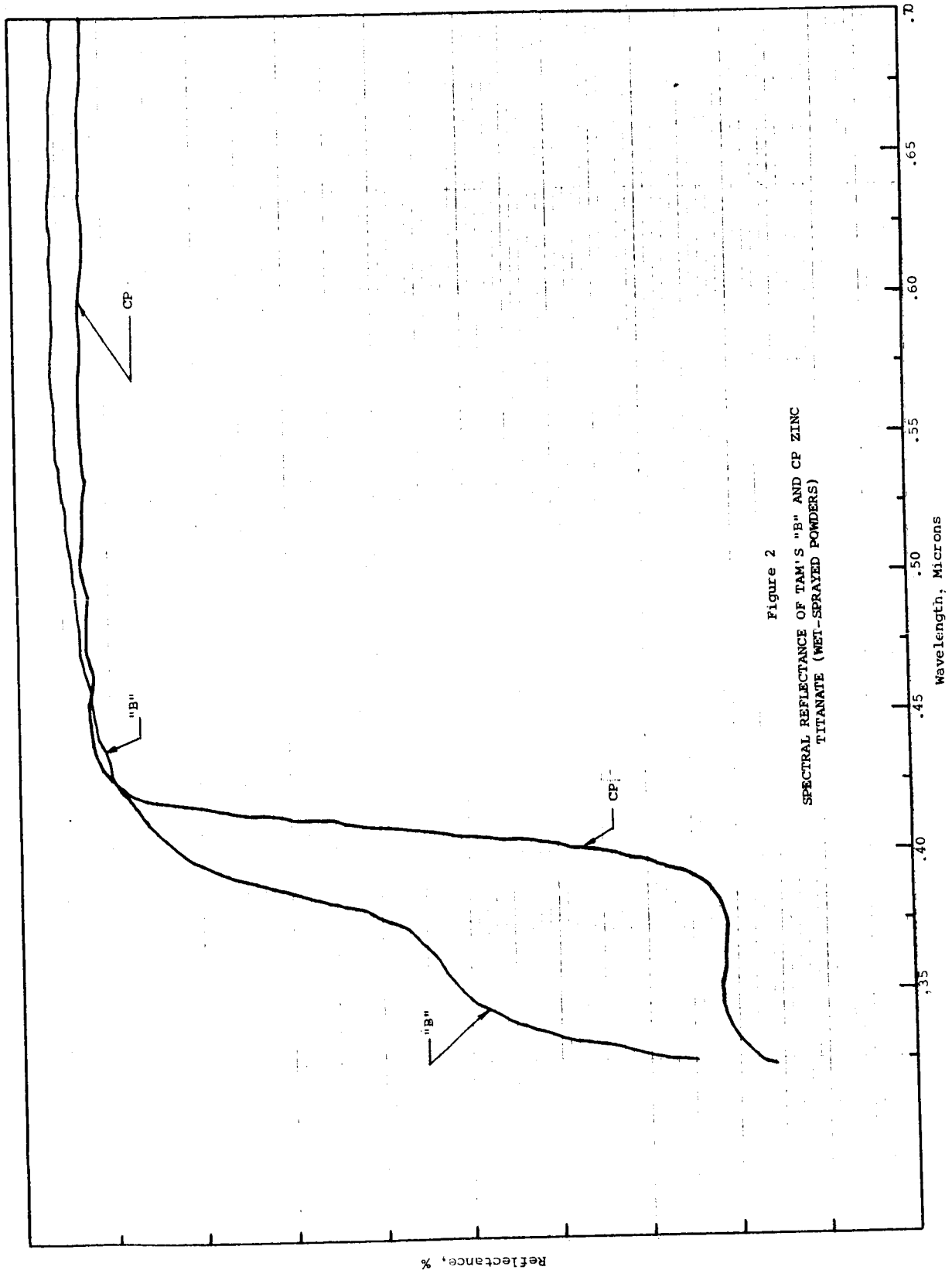

Figure 2

SPECTRAL REFLECTANCE OF TAM'S "B" AND CP ZINC TITANATE (WET-SPRAYED POWDERS)

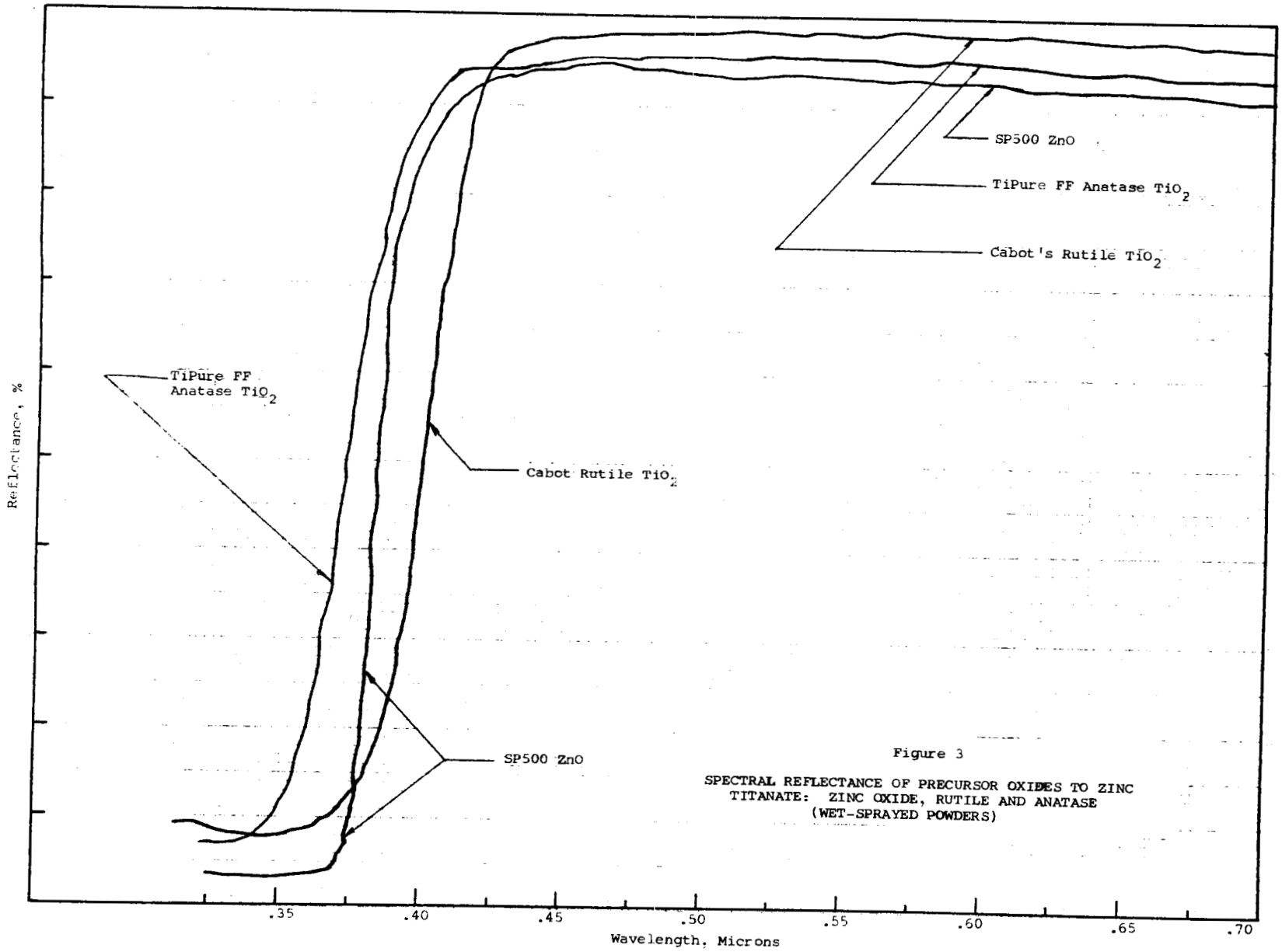

Figure 3

SPECTRAL REFLECTANCE OF PRECURSOR OXIDES TO ZINC TITANATE: ZINC OXIDE, RUTILE AND ANATASE (WET-SPRAYED POWDERS)

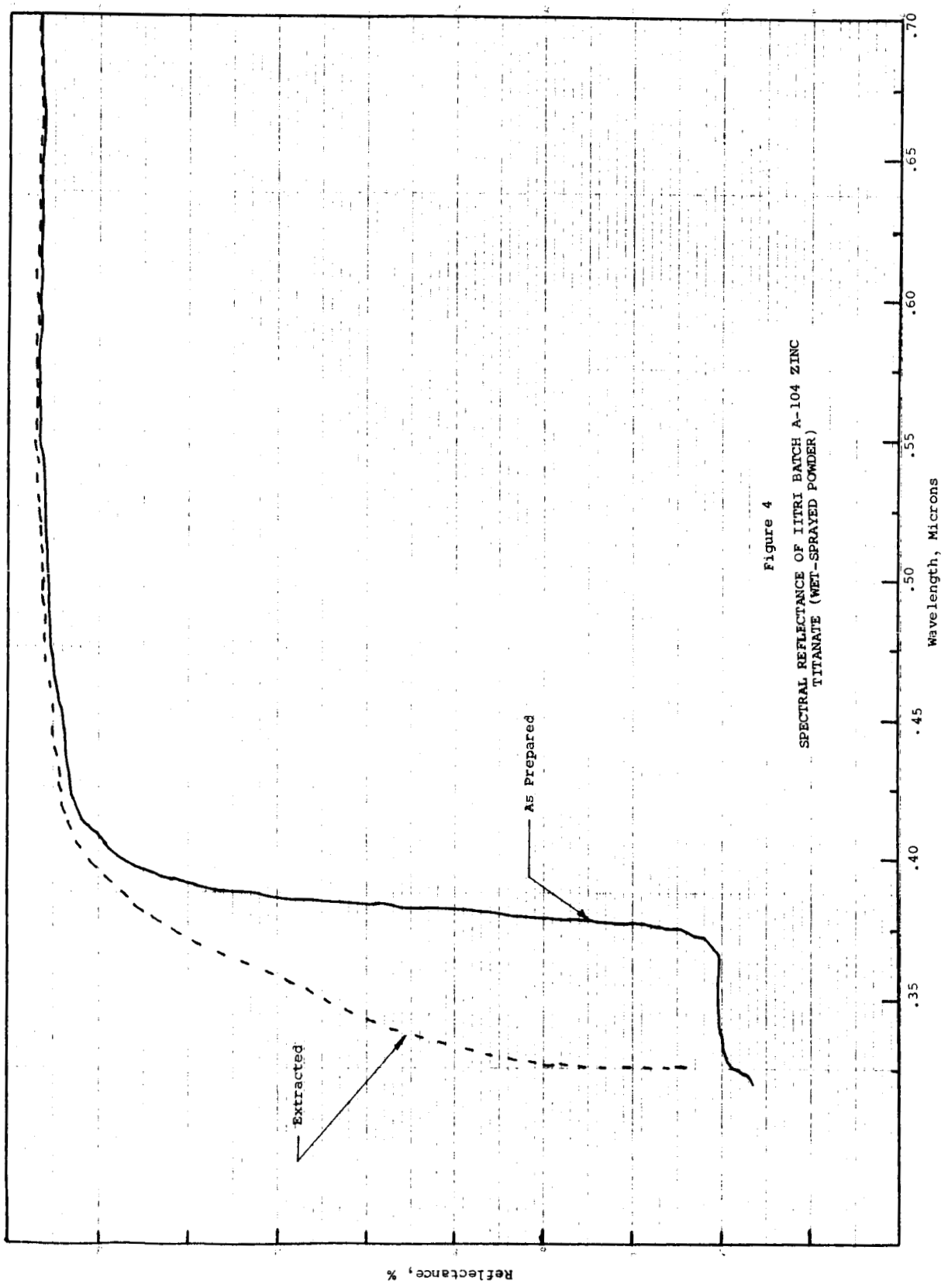

Figure 4

SPECTRAL REFLECTANCE OF IITRI BATCH A-104 ZINC TITANATE (WET-SPRAYED POWDER)

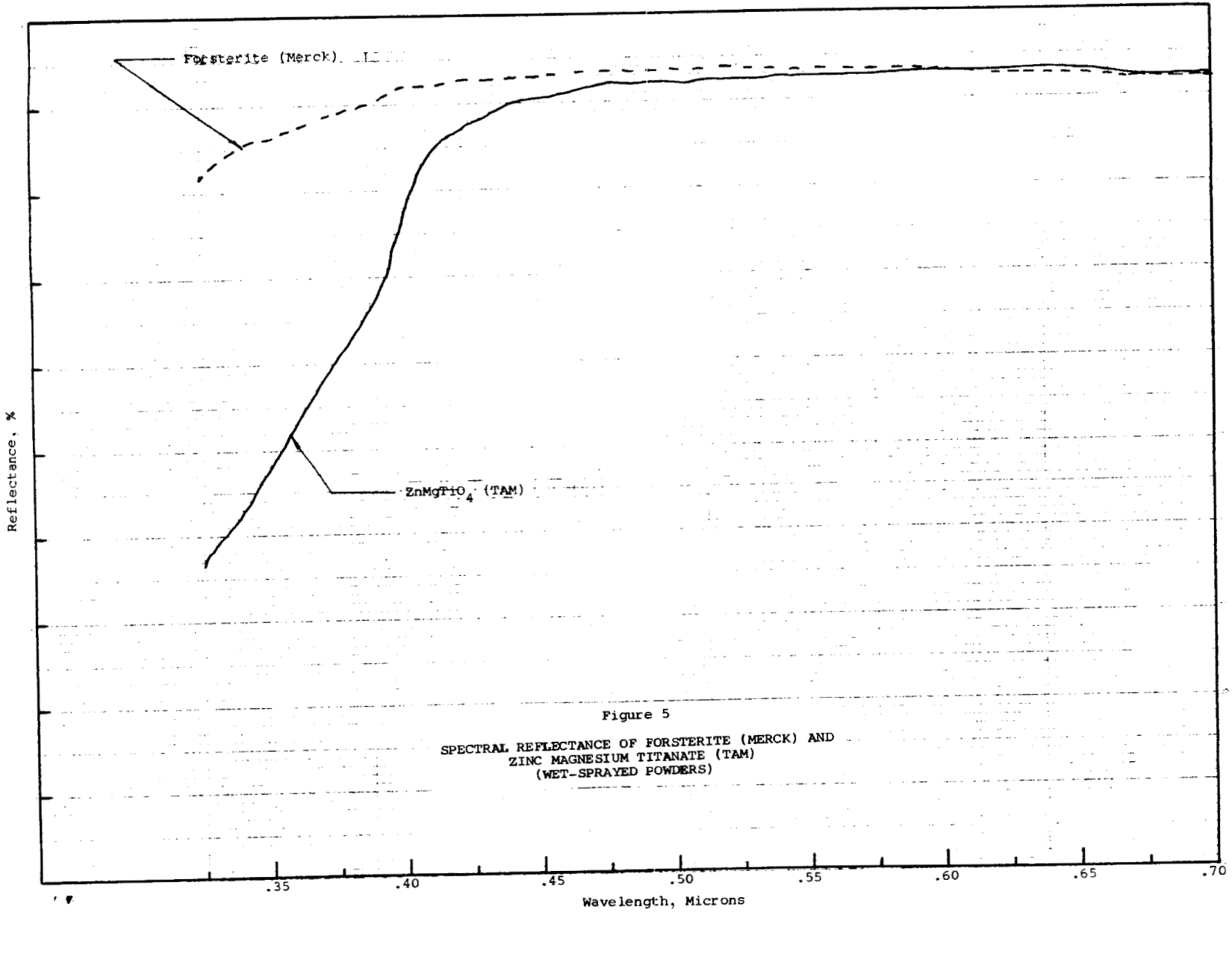

Figure 5

SPECTRAL REFLECTANCE OF FORSTERITE (MERCK) AND ZINC MAGNESIUM TITANATE (TAM) (WET-SPRAYED POWDERS)

The "step" in the reflectance spectra of batch A-104 at 3500 A was intrepreted as being due to unreacted zinc oxide. The zinc oxide was extracted from the A-104 specimen with acetic acid; 5.7% ZnO was found. The reflectance spectra of the A-104 pigment after extraction (Curve B in Figure 4) closely resembles that of New Jersey Zinc's A-54-2 zinc titanate (Figure 1). The higher reflectance shown by A-54-2 in the 3250- to 3800-A region may be due to differences in thicknesses of the two specimens. It is not known if the A-54-2 is extracted of if it represents more carefully controlled reaction conditions and proportions of the initial reactants.

A portion of batch A-104 was returned to the furnace and calcined for 2 more hours, this time at 900°C. The additional heating raised the "step" in the spectra from 20 to 37% reflectance at 3500-A wavelength (Figure 6). Extraction of ZnO with acetic acid produced a pigment which possessed an ultraviolet-reflectance spectra (Curve B in Figure 6) somewhat higher than than that exhibited by the A-54-2 specimen. However, as mentioned previously, it is very difficult to prepare powder specimens all at the same thickness and is even more difficult to measure the thickness of powder samples.

It was therefore concluded that 900°C is the minimum temperature required to produce a satisfactory pigment and that extraction of the unreacted zinc oxide is also essential.

Subsequent batches of zinc titanate were made at higher temperatures and for longer furnace times according to the schedule shown in Table 4. These syntheses resulted in lower unreacted zinc oxide residues and higher reflectances, particularly in the near ultraviolet region, but in all cases some zinc oxide still remained unreacted, confirming all previous references. Hence, extraction of residual zinc oxide is necessary to obtain the pigment desired.

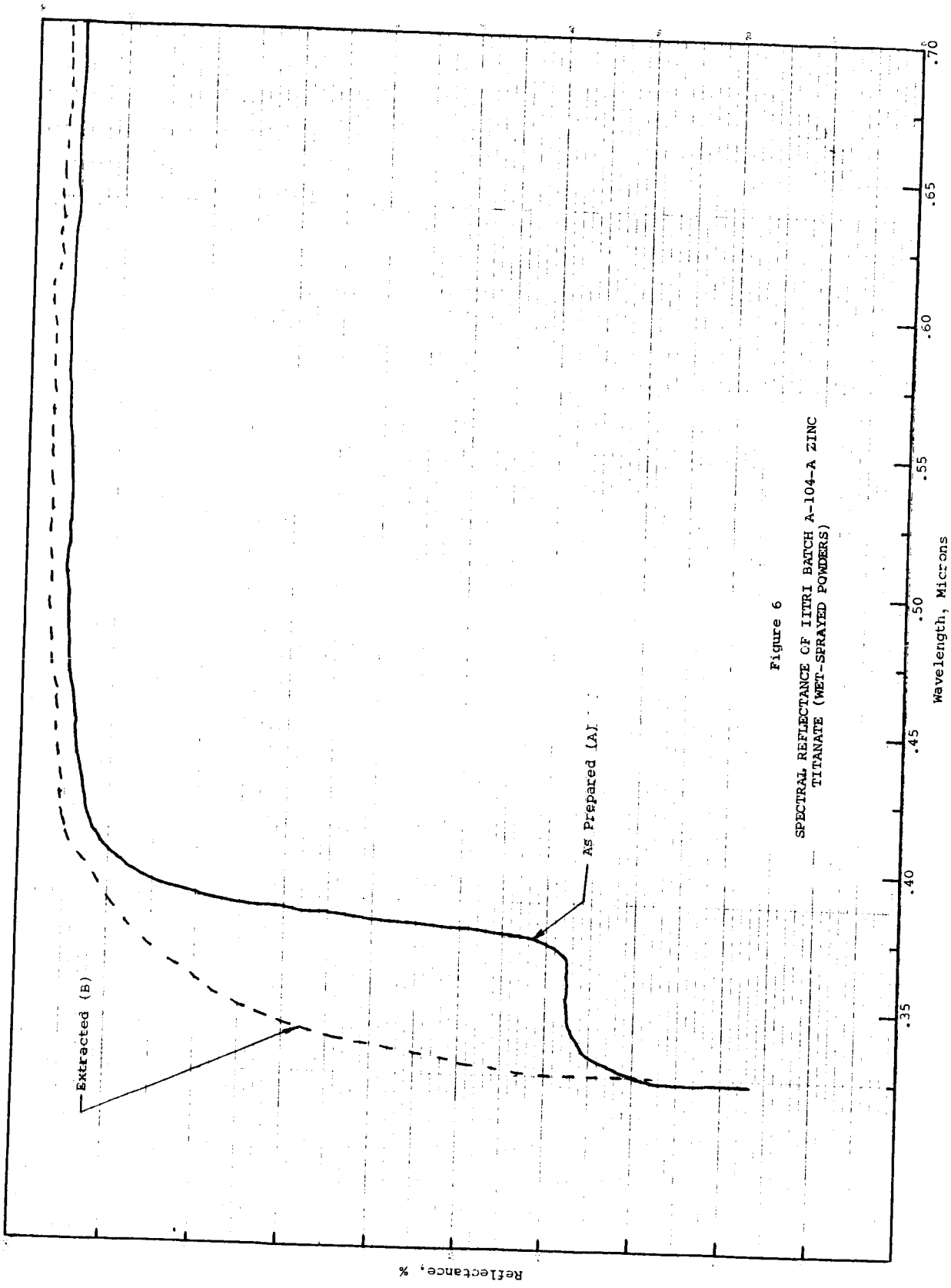

Figure 6

SPECTRAL REFLECTANCE OF IITRI BATCH A-104-A ZINC TITANATE (WET-SPRAYED POWDERS)

Table 4

SYNTHESIS SCHEDULE OF SEVERAL ZINC ORTHOTITANATES

Batch No.	Temperature, °C	Time Hrs	Not Extracted	Extracted	Reflectance (Figure No.)
A-111	800	16	X	X	7
A-111	910	18	X	X	8
A-114	1050	>16	X	X	9
A-115*	900	15	X	X	10

*Non-stoichiometric insofar as a slight excess of α-TiO_2 was used.

A sample of extracted zinc titanate pigment was analyzed by X-ray diffraction and the major composition was reported to be zinc orthotitanate, Zn_2TiO_4; however, some zincite was also present in spite of the extraction. This led to our questioning the efficiency of our zinc oxide-extraction process and the analytical procedure employed. We also questioned whether the orthotitanate was exactly what we wanted. A more efficient zinc oxide-extraction procedure was therefore developed and tested quantitatively as described in the Appendix. A re-survey of the literature was also made to find possible methods of forming other titanates.

Five zinc titanate batches of varying composition were prepared after a re-survey of the literature and after the new extraction procedures were developed. The pertinent information are contained in Table 5. One batch, A-129, was calculated to produce the maximum yield of metatitanate, $ZnTiO_3$. Two batches, A-130 and A-131, were devised to obtain the maximum yield of the sesquititanate, $Zn_2Ti_3O_8$. Similarly, batches A-132 and A-133 were intended to produce the maximum yield of the orthotitanate, Zn_2TiO_4.

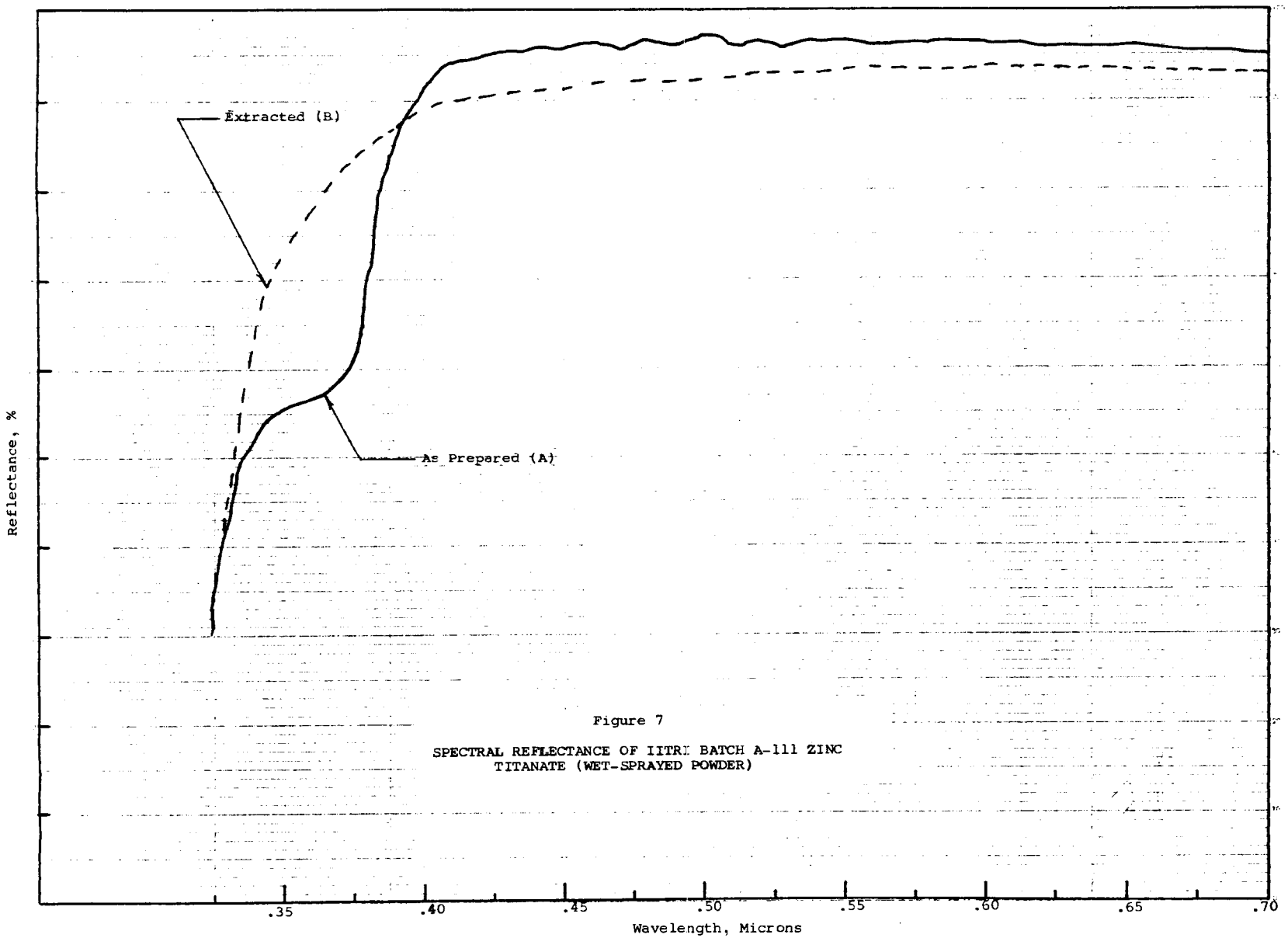

Figure 7

SPECTRAL REFLECTANCE OF IITRI BATCH A-111 ZINC TITANATE (WET-SPRAYED POWDER)

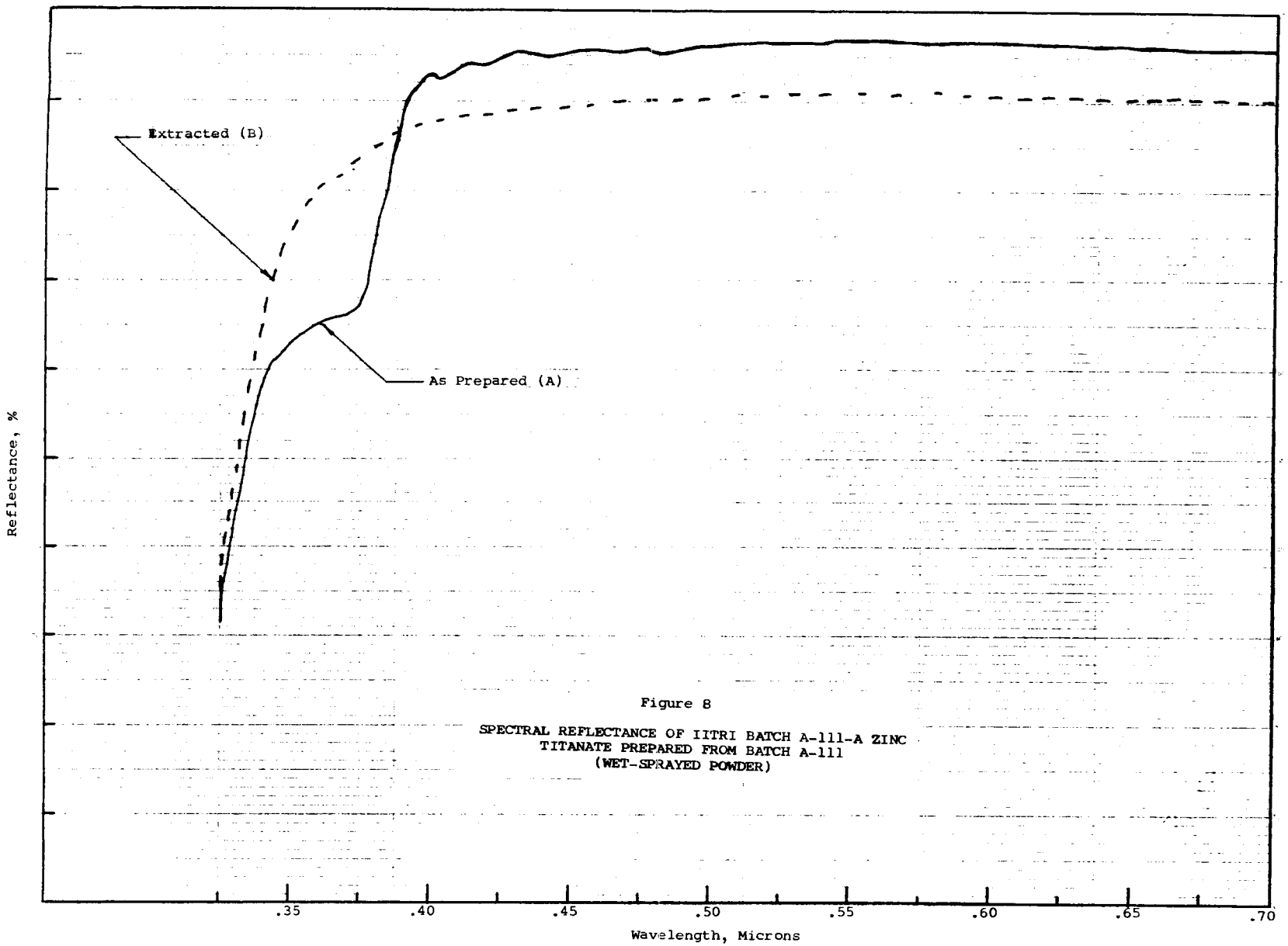

Figure 8

SPECTRAL REFLECTANCE OF IITRI BATCH A-111-A ZINC TITANATE PREPARED FROM BATCH A-111 (WET-SPRAYED POWDER)

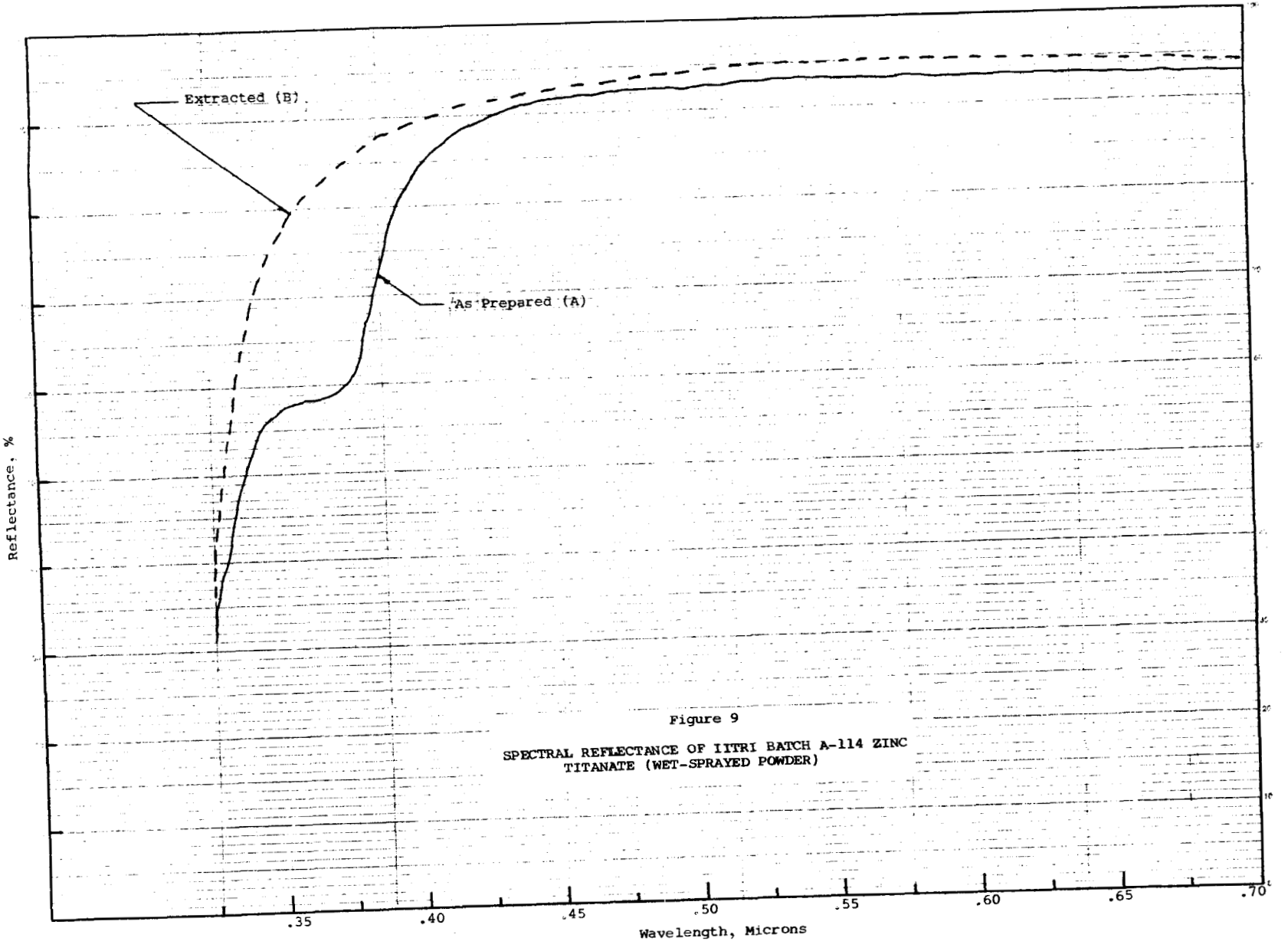

Figure 9

SPECTRAL REFLECTANCE OF IITRI BATCH A-114 ZINC TITANATE (WET-SPRAYED POWDER)

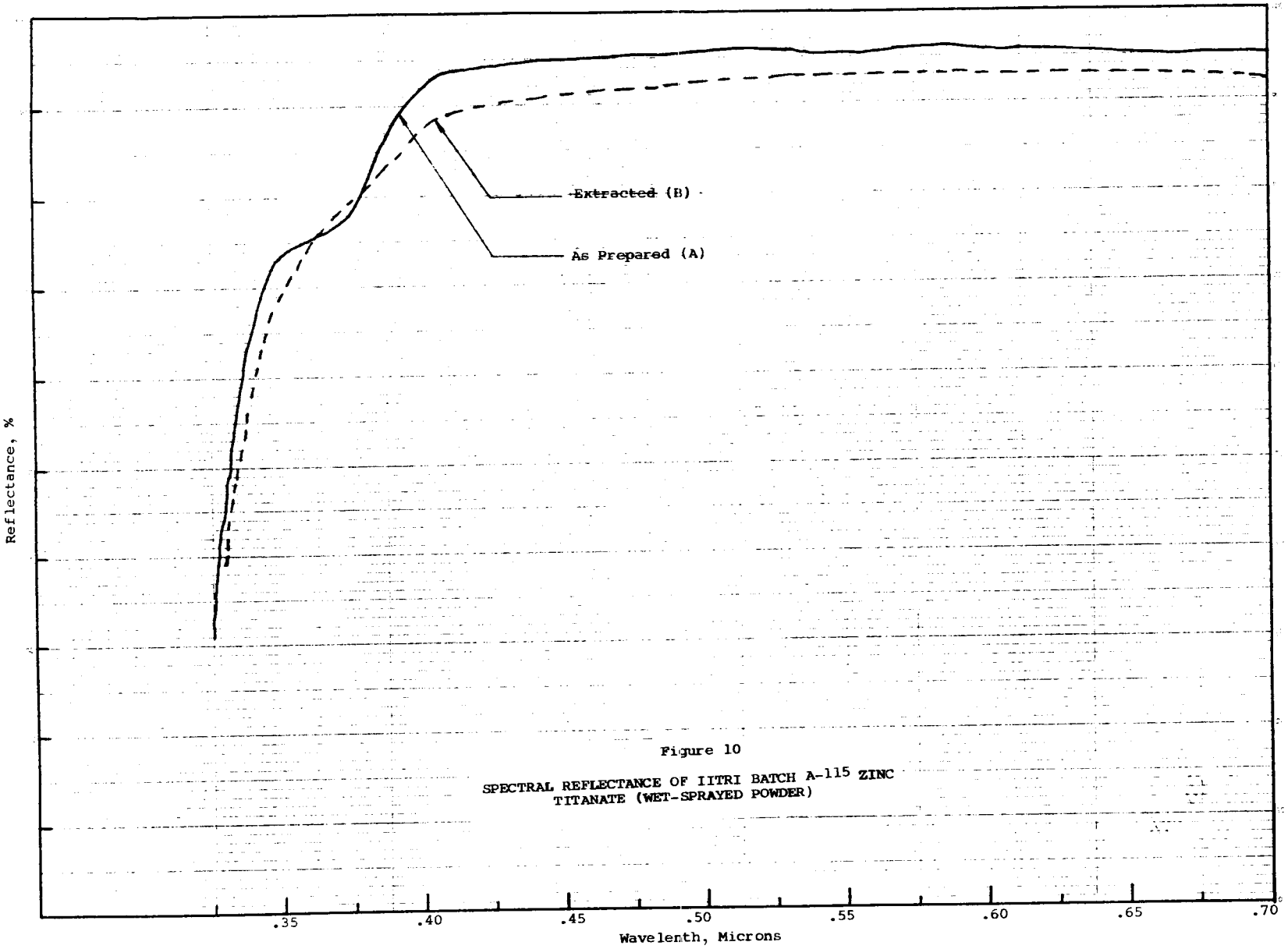

Figure 10

SPECTRAL REFLECTANCE OF IITRI BATCH A-115 ZINC TITANATE (WET-SPRAYED POWDER)

Table 5

SYNTHESIS SCHEDULE OF SEVERAL DIFFERENT ZINC TITANATES OF STOICHIOMETRY

Batch No.	Ratios of Reactants ZnO	Ratios of Reactants TiO_2	Temp. °C	Time Hrs	Structure	Reflectance (Figure No.)
A-129	1 mol	1 mol (rutile)	850	17	meta	11
A-130	1 mol	1 mol (anatase)	700	64	sesqui	12
A-131	2 mol	1 mol (anatase)	700	64	sesqui	13
A-132	2 mol	1 mol (anatase)	1050	17	ortho	14
A-133	3 mol	2 mol (anatase)	1050	17	ortho	15

Examination of the five pigments shown in Table 5 appear to confirm the existence of the three zinc titanates. Batch A-129, which was intended to produce zinc metatitanate, produced a very fine particle-sized, soft-textured, white pigment. On extraction with 10% acetic acid, only 0.785% zinc oxide was found and its extraction made absolutely no difference to the reflectance curve of the pigment (Figure 11). The reflectance spectra differed greatly from the other four and resembled somewhat that obtained from TAM's "CP" zinc titanate (Figure 2). The formation of this metatitanate is in good confirmation of the findings of Dulin and Rase (ref. 8) and Bartram and Slepetys (ref. 9). The X-ray diffraction pattern of this pigment has not been determined as yet, nor has that of TAM's "CP" zinc titanate. Stability under ultraviolet radiation at high vacuum and subsequent loss of reflectance, if any, still has to be determined. Hiding power (or tinting strength) of the pigment will also be obtained and compared to the original pigments from which it was made and to other batches of zinc titanate.

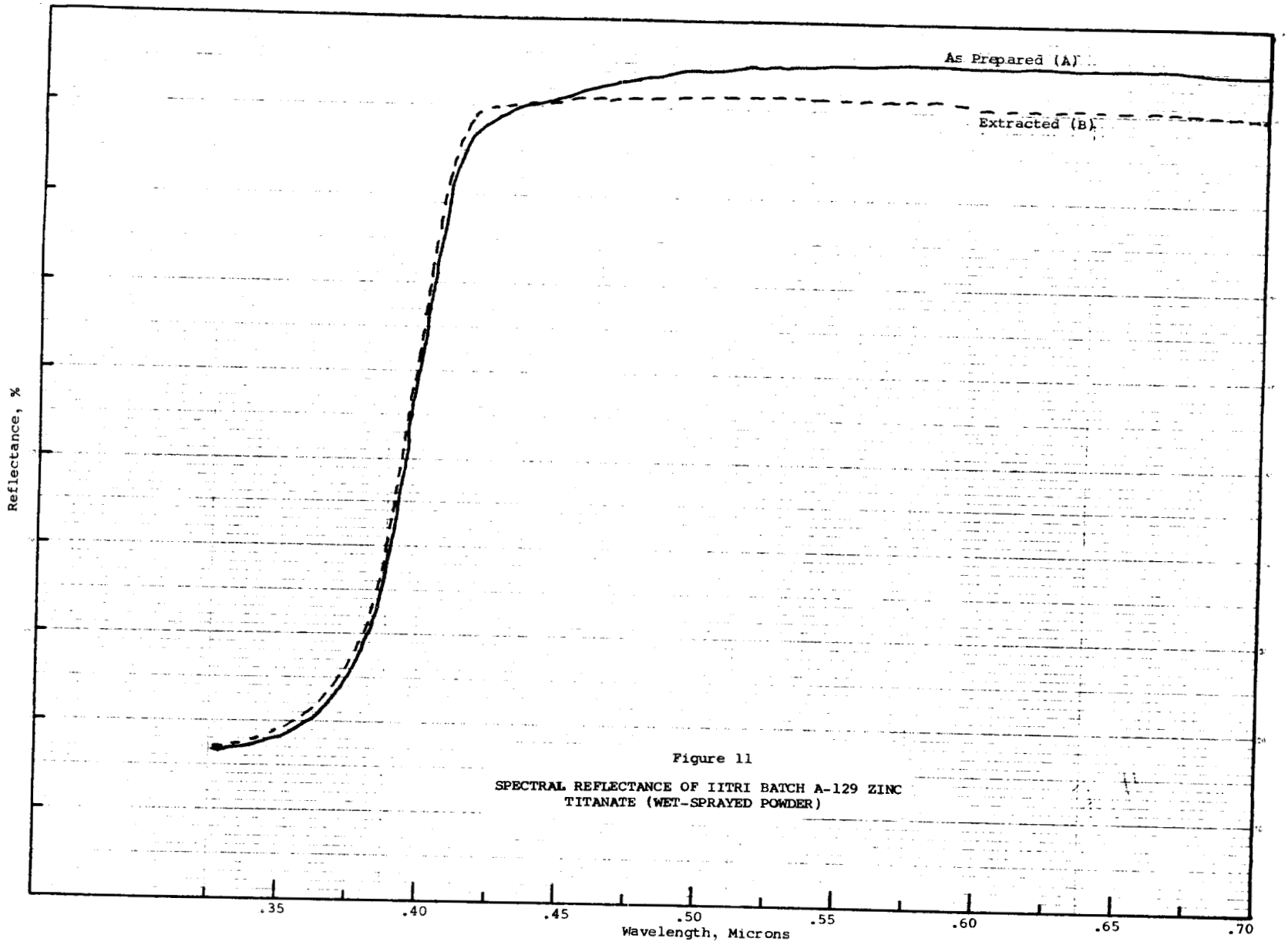

Figure 11

SPECTRAL REFLECTANCE OF IITRI BATCH A-129 ZINC TITANATE (WET-SPRAYED POWDER)

Batches A-130 and A-131, which were intended to produce the maximum yield of sesquititanate, also produced clean white pigments, soft in texture and low in unreacted zinc oxide. Batch A-130 showed 1.45% residual zinc oxide; batch A-131 showed 1.00% residual zinc oxide. The reflectance spectra for these two batches (Figures 12 and 13) are different from the orthotitanate and also different from the metatitanate. They reflect further into the ultraviolet than the metatitanate but by no means as far as the orthotitanate. Of the two, batch A-130 is slightly superior. An increase in ultraviolet reflectance, though slight, resulted from extraction of zinc oxide, but the shape of the curves did not change. This may be compared with the metatitanate where the extraction of the zinc oxide makes no difference whatever and with the orthotitanate where the extraction of the zinc oxide makes a very great difference, both in intensity of reflectance and in the shape of the spectral curve.

As in the case of batch A-129, the X-ray pattern has not been obtained for these pigments; the stability under ultraviolet radiation at high vacuum as well as the hiding power (or tinting strength) have yet to be determined.

In batches A-132 and A-133 which were orthotitanates calcined at 1050° the pigments show a slight yellowing and extreme hardness; they scratch glass. The Russian papers (ref. 7,10,11) list the hardness as 5 mho. Our impression, awaiting confirmation with a crystal of orthoclase, is that they exhibit a hardness of 6 mho. Batch A-132 is by far the superior of the two, being in complete accord with the literature. Although pigment A-132 shows the highest percentage of unreacted zinc oxide (2.2%), its spectra reflects the furthest into the ultraviolet prior to extraction; the step occurs at 57% reflectance. The step disappears entirely with the extraction of the 2.2% zinc oxide. The reflectance spectra of Batches A-132 and A-133 are presented in Figures 14 and 15, respectively.

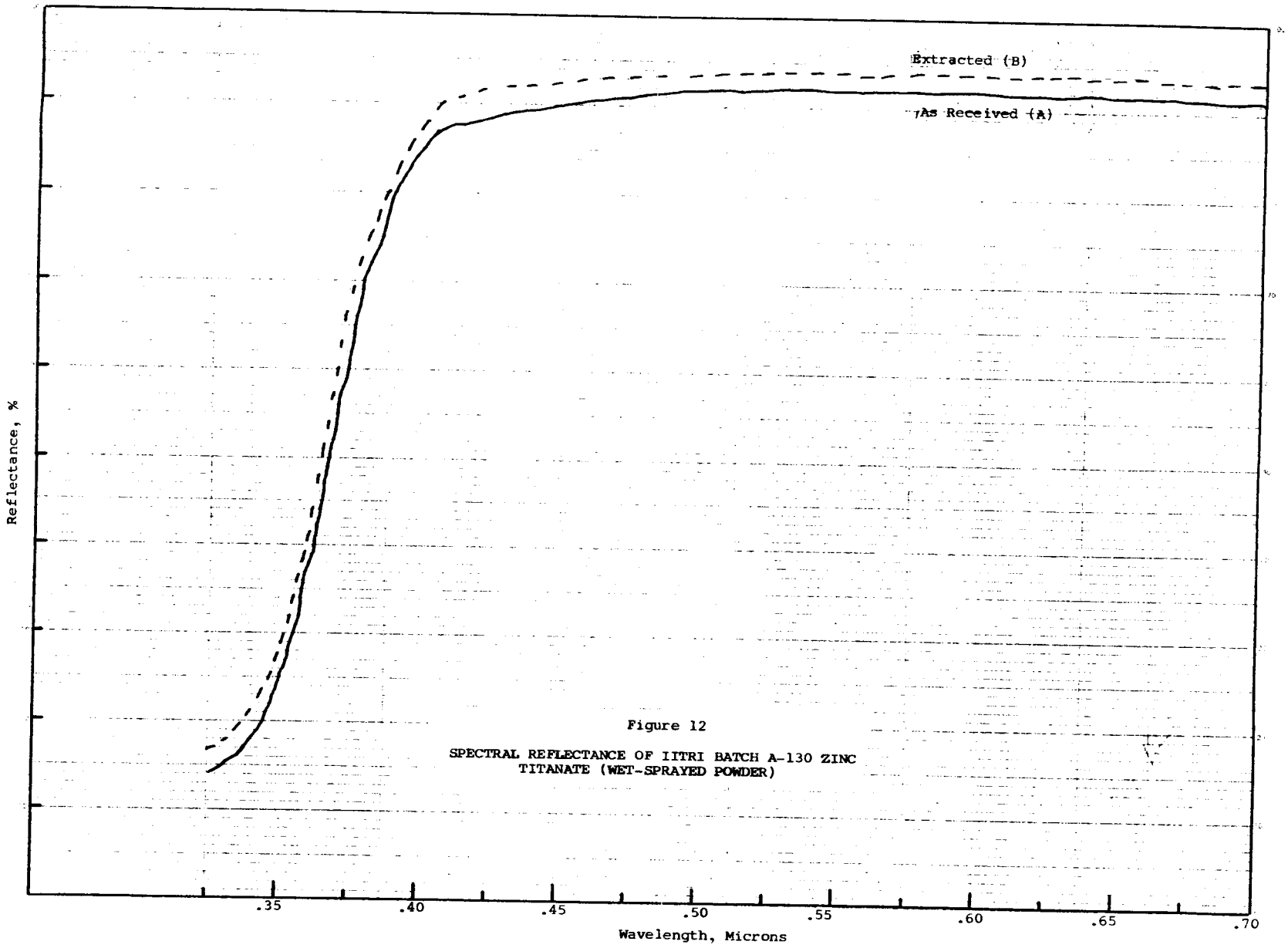

Figure 12

SPECTRAL REFLECTANCE OF IITRI BATCH A-130 ZINC TITANATE (WET-SPRAYED POWDER)

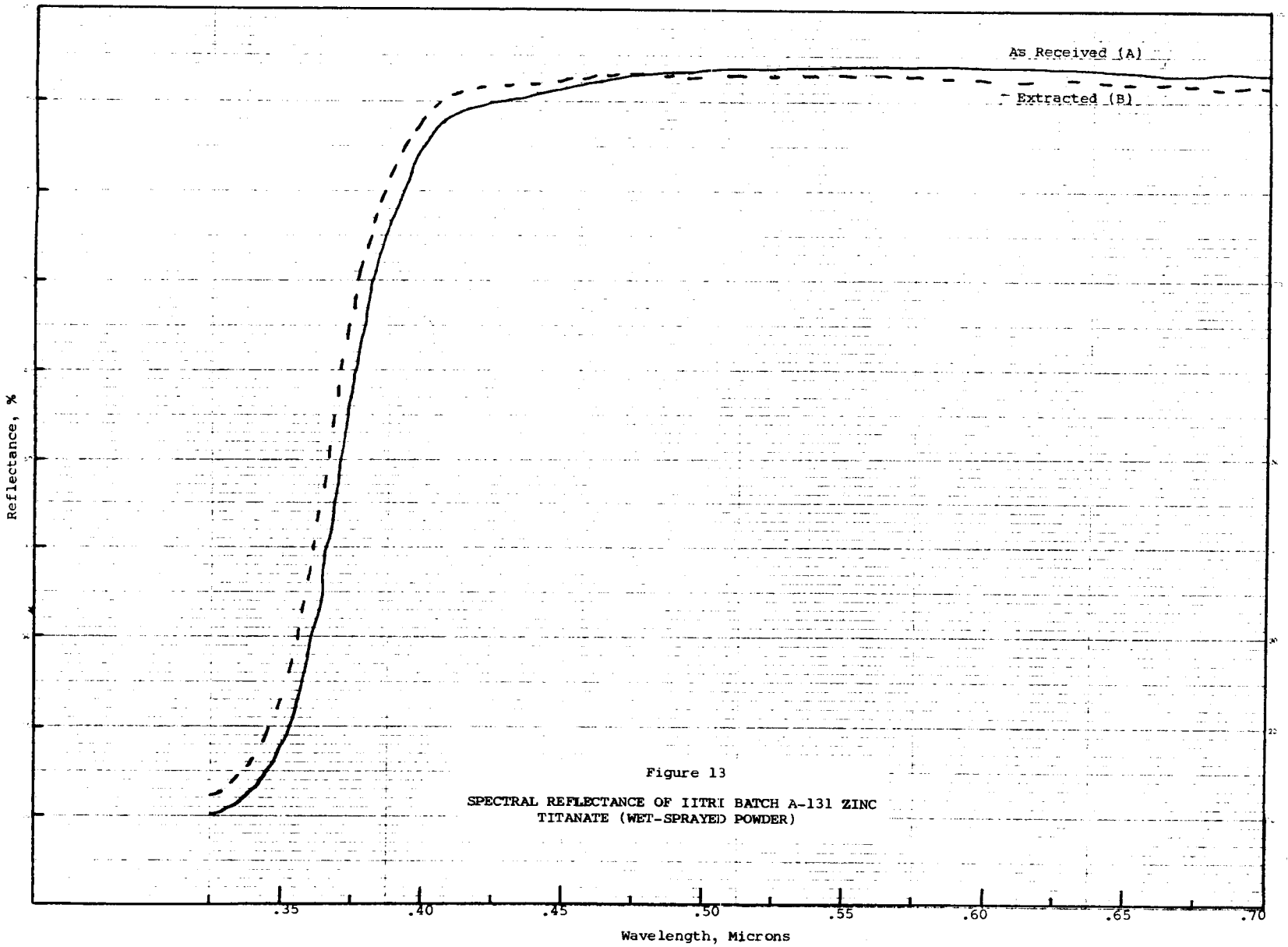

Figure 13

SPECTRAL REFLECTANCE OF IITRI BATCH A-131 ZINC TITANATE (WET-SPRAYED POWDER)

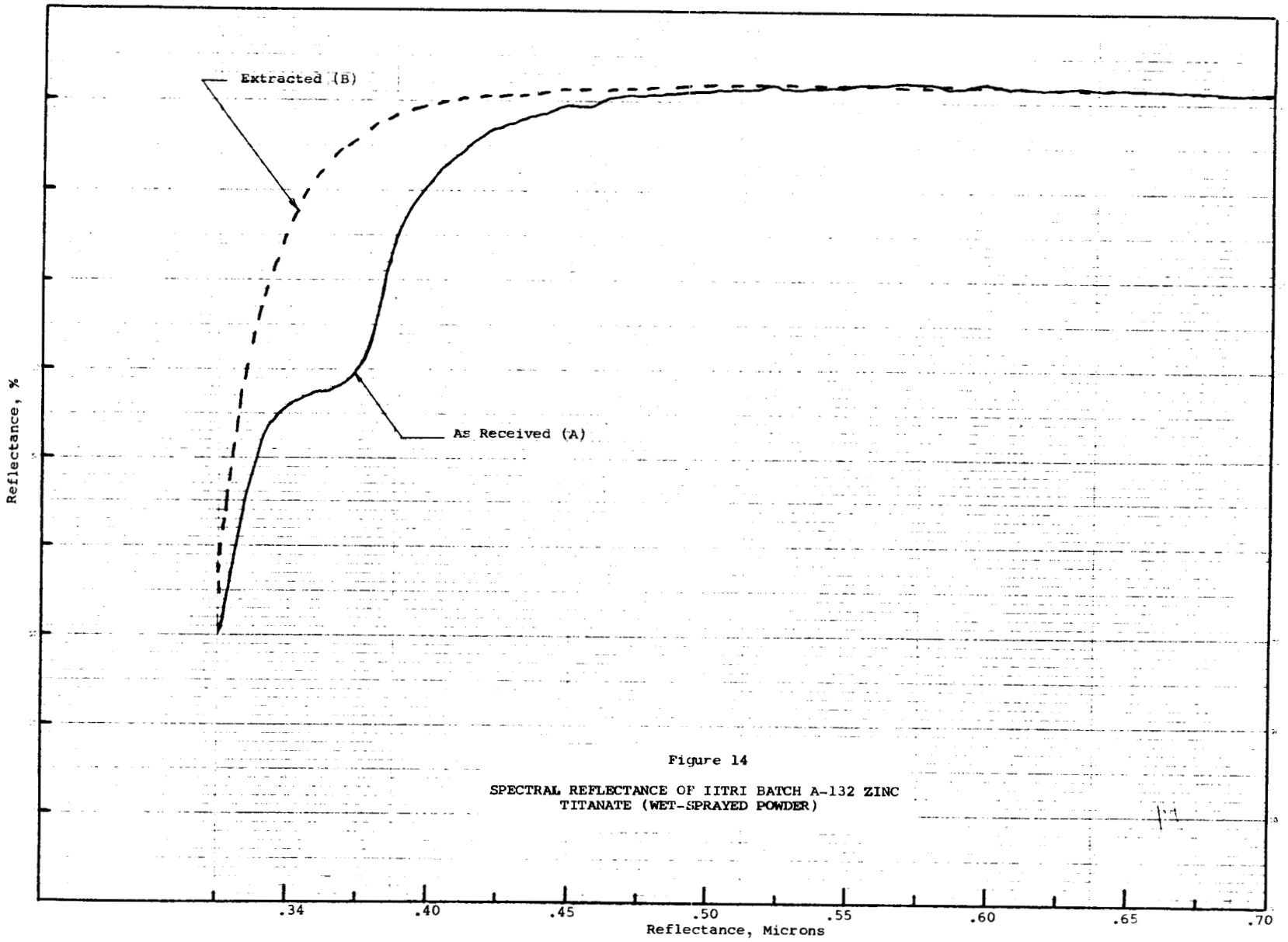

Figure 14

SPECTRAL REFLECTANCE OF IITRI BATCH A-132 ZINC TITANATE (WET-SPRAYED POWDER)

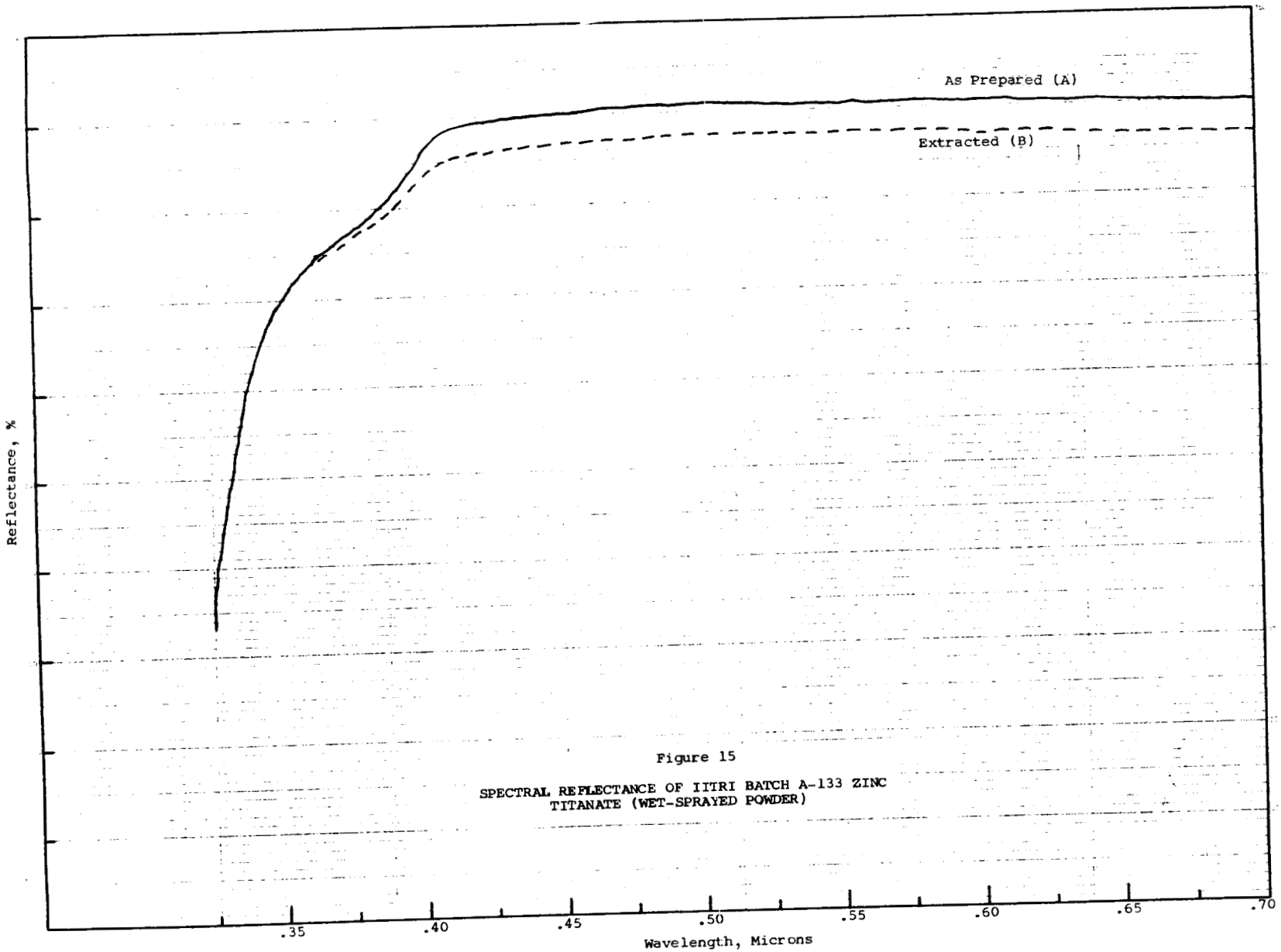

Figure 15

SPECTRAL REFLECTANCE OF IITRI BATCH A-133 ZINC TITANATE (WET-SPRAYED POWDER)

Extreme hardness may be a source of trouble in making commercial paint batches, but may be avoided by techniques employed in the calcining. The last two orthotitanate batches must also be analysed by X-ray diffraction: additionally, their hiding power and tinting strength will be determined. Their stability to ultraviolet under high vacuum is not expected to be any different from similar batches of orthotitanate, which have been excellent. Their stabilities will be determined however.

Some observation should be made at this point concerning the three commercial samples of zinc titanate: the A-54-2 of New Jersey Zinc Company and the "CP" and "B" zinc titanate from TAM.

From the reflectance spectra (Figures 1 and 2), the A-54-2 is definitely an orthotitanate with not more than a slight trace of zinc oxide present. The TAM "CP" zinc titanate appears definitely to be metatitanate, although we have not analyzed it for composition as yet. The TAM zinc titanate "B" appears to be either a sesquititanate or a mixture of sesqui and orthotitanates. It will be necessary to analyze these commercial samples by X-ray diffraction at the time we determine the batches listed above. We also intend to extract the free zinc oxide, if any, and to find what difference this produces in the reflectance spectra and in ultraviolet stability.

4. Space-Ultraviolet Simulation Tests on Zinc Titanate Powders

The stability of several zinc titanate powders, forsterite, SP500 zinc oxide and zinc magnesium titanate to 1000-ESH of ultraviolet irradiation in vacuum was determined in Test Q-22. Test Q-22 involved post-exposure reflectance measurements employing the Edwards-type integrating-sphere attachment for the Beckman DK-2A. The test was for 1000-ESH at about 6 solar intensities. A computor program has not yet been completed to accomplish the reduction of data obtained on the "absolute" attachment for the DK-2A. The spectral data are presented, however, in Table 6 for six wavelengths. The data show the excellent stability of

Table 6

EFFECT OF 1000-ESH UV ON THE REFLECTANCE OF SEVERAL PIGMENT POWDERS[1]

Specimen	Material	ESH[2]	Absolute Hemipsherical Reflectance Wavelength, Microns 0.35	0.40	0.45	0.70	1.0	2.0
5279	$ZnMgTiO_3$	0	45.0	73.0	87.5	90.8	91.3	88.8
		1000	42.0	68.0	78.2	89.7	91.0	88.0
5280	Forsterite	0	82.8	90.2	92.9	91.5	91.0	88.8
		1000	37.6	50.2	63.0	88.0	90.7	88.2
5281	Zn_2TiO_4 (A-54-2)	0	75.0	88.8	92.0	94.4	95.3	92.9
		1000	73.8	86.2	88.0	90.0	90.0	88.2
5282	Zn_2TiO_4 (A-111-A)	0	56.2	88.2	92.0	92.8	93.8	92.3
		1000	55.8	88.0	91.2	92.3	93.5	91.3
5283	A-111-A Extracted	0	71.5	84.9	87.3	88.0	88.5	88.3
		1000	70.0	82.0	85.2	87.5	88.2	87.1
5284	NS Zn_2TiO_4[3] (A-115)	0	71.0	90.3	93.8	94.0	94.5	93.0
		1000	70.0	89.0	92.0	93.7	94.5	92.4
5285	A-115 Extracted	0	74.0	88.8	92.0	92.3	92.4	91.4
		1000	72.0	85.5	89.5	91.5	92.0	90.3
5286	SP500 ZnO	0	4.2	84.5	92.5	90.5	88.5	86.7
		1000	2.8	83.5	91.5	89.8	87.2	85.2

[1]Test Q-22

[2]1000 ESH at about 6X solar intensities

[3]Non-Stoichiometric (i.e., excess α-TiO_2)

the zinc titanate powders; the data also indicate that the synthetic forsterite is very unstable and the zinc magnesium titanate is too unstable to be further considered at this time. The $ZnMgTiO_3$ was obtained from TAM and the forsterite from Merck, Inc.

The slight degradation that is shown in the infrared by the New Jersey Zinc specimen, 5281, cannot be explained at this time. Furthermore, the acetic-acid extracted experimental zinc titanates (5282 and 5284) exhibited slightly inferior stability in the 0.35- to 0.45-μ region compared to the unextracted specimens (5283 and 5285). This may be due to the absence of protective zinc oxide and/or to residual acetic acid contamination. Further studies are planned to elucidate this possibility.

III. METHYL SILICONE PAINTS

A. Simulation Tests Employing Post-Exposure Measurements

The results of two 2000-ESH space-simulation tests, Q-20 and Q-21, on A-54-2 zinc titanate-pigmented silicone coatings are presented in Table 7. Specimens 5266 and 5267 are prepared from Owens-Illinois Type 901 glass resin and GE's RTV-602 silicone, respectively. The excellent stability of both the A-54-2 Zn_2TiO_4 and the O-W 901 resin are manifested in the $\Delta\alpha$ of only 0.027 exhibited by this coating when irradiated for over 2000 ESH. The initial solar absorptance of 0.115 is the lowest we have ever recorded for a non-inorganic coatings.

The poor stability exhibited by specimen 5267, a zinc titanate-pigmented RTV-602, is attributed to the addition of excessive catalyst. The formulation requires the addition of 0.5% SRC-05 catalyst based upon the weight of RTV-602; a concentration of 5% was erroneously added, however. The excessive catalyst was also thought to be responsible for the initial α_s of 0.147, which is higher than expected from previous studies.

The specimen (5271) of A-54-2 zinc titanate-pigmented RTV-602 irradiated in Test Q-21 was catalyzed with 0.4% SRC-05 catalyst and compares very favorably with the specimen (5267) irradiated in Test Q-20. Excellent stability of the A-54-2 zinc titanate-pigmented Owens Illinois 650 resin is shown by two specimens, 5272 and 5273. The $\Delta\alpha$'s for the two specimens were 0.015 and 0.010, respectively. The initial solar absorptance of 0.18 is higher than anticipated and is attributed to thin samples and non-optimum pigment volume concentration.

B. Solubility Studies of Silicone Resins

1. General Electric's RTV-602

The solubility characteristics of General Electric's RTV-602 silicone potting material, which is used as the vehicle in the S-13 and S-13G zinc oxide paints and in our recent zinc titanate formulations, was determined employing a wide variety

Table 7

RESULTS OF 2000 ESH SIMULATION TEST ON SEVERAL ZINC TITANATE-PIGMENTED SILICONE PAINTS

Specimens	Material	Test No.	Exposure[1] (ESH)	Solar Absorptances α_1	α_2	α_s	Δ_α
5266	Zn_2TiO_4 OW901	Q-20	0	.062	.053	.115	-
			2000	.088	.054	.142	.027
5267	Zn_2TiO_4[2] RTV602	Q-20	0	.083	.064	.147	-
			2000	.127	.070	.197	.050
5271	Zn_2TiO_4 RTV602	Q-21	0	.071	.053	.124	-
			2000	.090	.059	.149	.025
5272	Zn_2TiO_4 OW650	Q-21	0	.088	.095	.183	-
			2000	.100	.098	.198	.015
5273	Zn_2TiO_4 OW650	Q-21	0	.087	.092	.179	-
			2000	.094	.095	.189	.010

[1] 2000 ESH at ~7 solar intensities

[2] Excessive SRC-05 catalyst used

of solvents and diluents. The results of these tests are presented in Table 8; these experiments involved flow-out tests on glass plates.

While RTV-602 is quite soluble in a variety of solvents, a smooth pour, free from "crawling," "ridging," discontinuous breaks, and "rainbow" bands was observed using the following single solvents only; isopropanol, isopropyl acetate and isopropyl ether. The diluent petroleum ether (which is not a solvent) also resulted in a smooth film.

The isopropyl ether gave the best solution and film but resulted in extremely rapid evaporation and was, therefore, too fast to handle. Based upon these tests, a thinner was formulated as follows:

50% Isopropanol
25% Petroleum ether
25% Isopropyl acetate

Although use of this thinner in place of the toluene resulted in a highly superior film compared to toluene/RTV-602 films, this thinner formulation appeared to preclude satisfactory curing by destroying the effectiveness of the catalyst. We have therefore returned to toluene with a small percentage of isopropanol (10%) and n-butyl acetate (5%) added to give a lower viscosity and smoother spray with S-13 paints.

2. Owens-Illinois Type 650 Glass Resin

The type 650 glass resin is supplied at 40% solids in normal butanol. It is fully soluble in, and gives a smooth flow-out over glass and metals, when poured from the following solvent combinations:

5 parts of the 40% solution of 650 in butanol
3 parts of either of the following solvents:

a. isopropanol
b. isopropyl acetate
c. methyl isobutyl ketone
d. cellosolve
e. isopropyl ether

Table 8

SOLUBILITY OF RTV-602 IN VARIOUS SOLVENTS

Group	Solvent	Solution	Film
Hydrocarbons	Light petroleum ether	Insoluble	(Even, smooth)
	Benzine	Borderline, colloidal suspension or gel	Shrinkage or creep-up of the pour, rainbow fringes
	Benzene	Soluble	Shrinkage or creep-up of the pour, rainbow fringes
	Toluene[a]	Soluble	Shrinkage or creep-up of the pour, slight rainbow fringes
	Xylene	Soluble	Shrinkage or creep-up of the pour, rainbow fringes
	Turpentine	Soluble	Shrinkage or creep-up of the pour, rainbow fringes
Alcohols	Methanol	Insoluble	
	Ethanol, 190p	Insoluble	
	Ethanol, 200p	Insoluble	
	Isopropanol[a]	Soluble	Discontinuous pour, even, smooth
	Butanol	Soluble	Shrinkage or creep-up of the pour, rainbow fringes, discontinuous pour
	Methyl isobutyl carbinol	Excellent	Rainbow fringes, discontinuous pour
	Diisobutyl carbinol	Excellent	Rainbow fringes, discontinuous pour
Ketones[b]	Acetone	Insoluble	Discontinuous pour
	Methyl ethyl ketone	Soluble	Rainbow fringes
	Methyl isobutyl ketone	Soluble	Rainbow fringes
	Diethyl ketone	Soluble	Rainbow fringes
	Diisobutyl ketone	Soluble	Rainbow fringes
	Diacetone	Borderline, colloidal suspension or gel	Rainbow fringes
	Isophorone	Insoluble	
	Cyclohexane	Insoluble	
Acetates	Ethyl acetate	Soluble	Rainbow fringes
	Isopropyl acetate[a]	Excellent	Even, smooth
	n-Butyl acetate	Soluble	Rainbow fringes
	Amyl acetate	Soluble	Rainbow fringes
	Methyl amyl acetate	Soluble	Rainbow fringes
	Methyl cellosolve acetate	Insoluble	Discontinuous pour
	Cellosolve	Borderline, colloidal suspension or gel	Discontinuous pour
	Butyl acetate	Insoluble	Discontinuous pour

Table 8 (cont.)

Group	Solvent	Solution	Film
Miscellaneous	Methyl cellosolve	Insoluble	Discontinuous pour
	Cellosolve	Borderline, colloidal suspension or gel	Discontinuous pour
	Butyl cellosolve	Borderline, colloidal suspension or gel	Discontinuous pour
	Dioxane	Borderline, colloidal suspension or gel	Discontinuous pour
	2-Nitropropane	Insoluble	
	Isopropylether	Excellent	Very smooth

[a]Best of group.

[b]None of the ketones is a good solvent.

This is the solvent combination presently being used to prepare paints based on the Owens-Illinois Type 650 Glass Resin.

3. Owens-Illinois Type 901 Glass Resin

The results of solubility studies employing numerous hydrocarbon and alcohol solvents are presented in Table 9. Additional tests showed that, except for cyclohexanone, all ketones are ineffective as solvents (or diluents), as are all esters and ethers employed. Cellosolve and methyl cellosolve solubilize the Type 901 Glass Resin, however. On the basis of these tests, a mixed thinner of toluene with butanol, MIBC or cellosolve is recommended.

Table 9

SOLUBILITY OF OWENS-ILLINOIS GLASS RESIN 901

Group	Solvent	Solution	Film
Hydrocarbons	Light petroleum ether	Insoluble	(Even smooth)
	Benzine	Insoluble	(Even smooth)
	Benzene	Border line, colloidal suspension or gel	Rainbow fringes
	Toluene	Border line, colloidal suspension or gel	Rainbow fringes
	Xylene	Border line, colloidal suspension or gel	Rainbow fringes
	Turpentine	Border line, colloidal suspension or gel	Rainbow fringes
Alcohols	Methanol	Soluble	Rainbow fringes
	Ethanol 190p	Soluble	Rainbow fringes
	Ethanol 200p	Soluble	Rainbow fringes
	Isopropanol	Soluble	Rainbow fringes
	n-Butanol	Soluble	Shrinkage or creep-up of the pour, dull
	MIBC	Soluble	Best

IV. SILICONE PHOTOLYSIS STUDIES

A. Introduction

The objective of this phase of the program is the synthesis of methyl silicone polymers that are totally resistant to solar radiation. This phase of the research program has received the lowest priority of the numerous tasks assigned and no work was performed during the first nine months of the calendar year. This inactivity resulted from (1) the necessity to divert time and monies to the problem of in situ-measurement of optical properties, (2) a funding lapse of several weeks earlier in the year and (3) a long delay in obtaining the necessary adaptor that was required to perform the irradiations within the mass spectrometer's pumping system.

The immediate objectives of this task are (1) to determine the inherent stability of the basic silicone structure, (2) to determine the mechanism of the ultraviolet-degradation processes, (3) to assess the influence of various side-chain or substitutent groups, and (4) to assess the influence of contamination on the photolytic processes and to identify those contaminants which promote or otherwise affect polymer degradation.

It was planned that ultraviolet photolyses of silicone polymers would be followed by (1) ultraviolet (differential) absorption spectroscopy, (2) mass spectrometry and (3) electron-spin-resonance spectroscopy. The ultraviolet spectroscopy experiments were not performed during this report period due to the decision to construct an irradiation facility which would employ the in situ measurement of spectral transmittance in the 0.2- to 1.0-micron wavelength region. This facility is currently being constructed by NASA-Marshall Space Flight Center, the sponsoring agency, and will be available for use on the program during the next calendar year.

Twelve polymer (methyl silicone) specimens were irradiated with ultraviolet in vacuum about one year ago. The results of these tests are summarized in Triannual Report IITRI-U6002-31 (November 9, 1965). The mass spectrometer and apparatus employed in these earlier tests are described in Triannual Report IITRI-C6014-26 (July 20, 1965).

The irradiation experiment described in this report was performed on apparatus shown in Figures 16 through 19. Figures 16 through 18 are schematics of the irradiation train that is affixed to the Hitachi RMU-6D mass spectrometer, which is shown in Figure 19. The spectrometer is single focussing (M/dM = 2000) and equipped with an electron-multiplier detector for high-sensitivity detection (fractions of a ppm). Compounds with molecular weights up to 1500 can be analyzed with unit resolution. Mass spectrograms are produced on an ascillographic recorder providing rapid recording at high scan rates (m/e of 12-500 in 3 sec).

The electron-spin-resonance spectrometer is shown in Figure 20.

B. Irradiation Procedure and Analysis of Mass Spectra

The Suprasil I electron-spin-resonance tubes shown in Figures 16-18 were filled with the silicone resin under investigation. This resin was a liquid specimen (LP-5) of low molecular weight methyl silicone polymer with a Me/Si mol ratio of 1.6. The polymer was prepared in diethyl ether and the raw material possessed a slight odor of ether when charged to the irradiation tubes.

The samples of liquid silicone polymer were evacuated overnight at room temperature using the pumping system of the mass spectrometer. The lowest pressure attainable after pumping overnight was approximately 1×10^{-5} torr, indicating that the polymer had a vapor pressure of approximately 10^{-5} torr at room temperature.

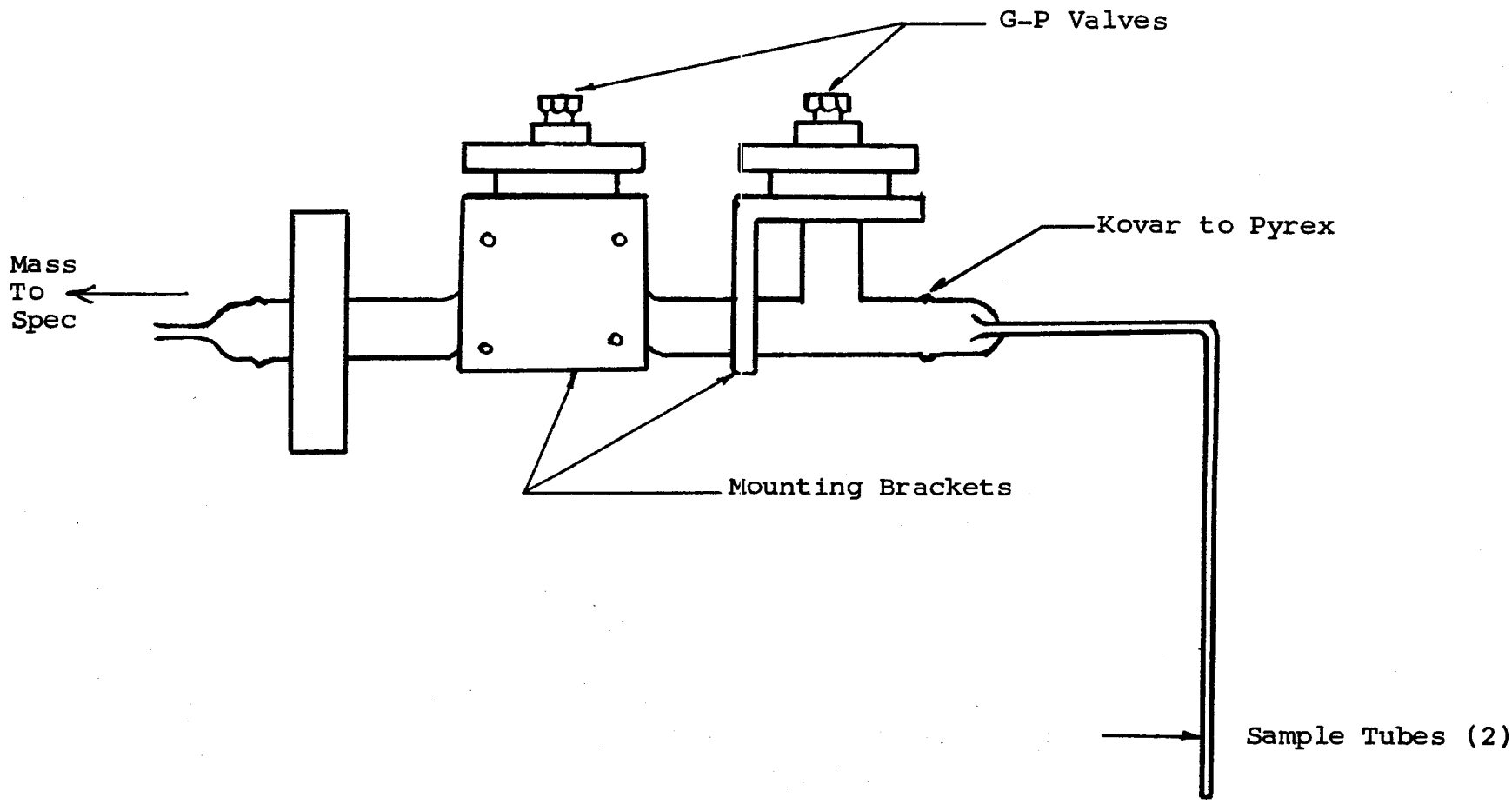

Figure 16

SCHEMATIC (SIDE VIEW) OF THE PHOTOLYSIS TRAIN

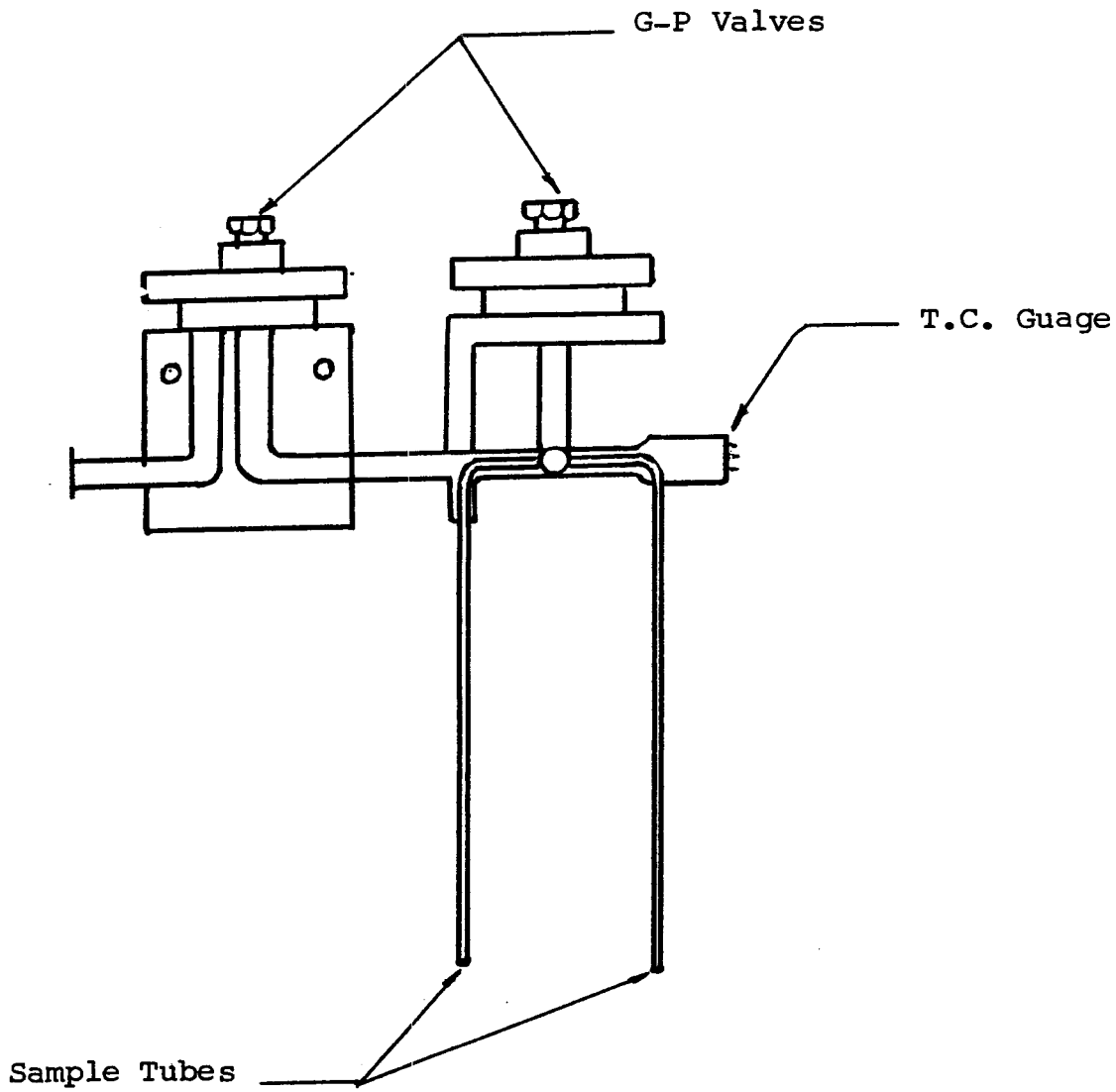

Figure 17

SCHEMATIC (END VIEW) OF THE PHOTOLYSIS TRAIN

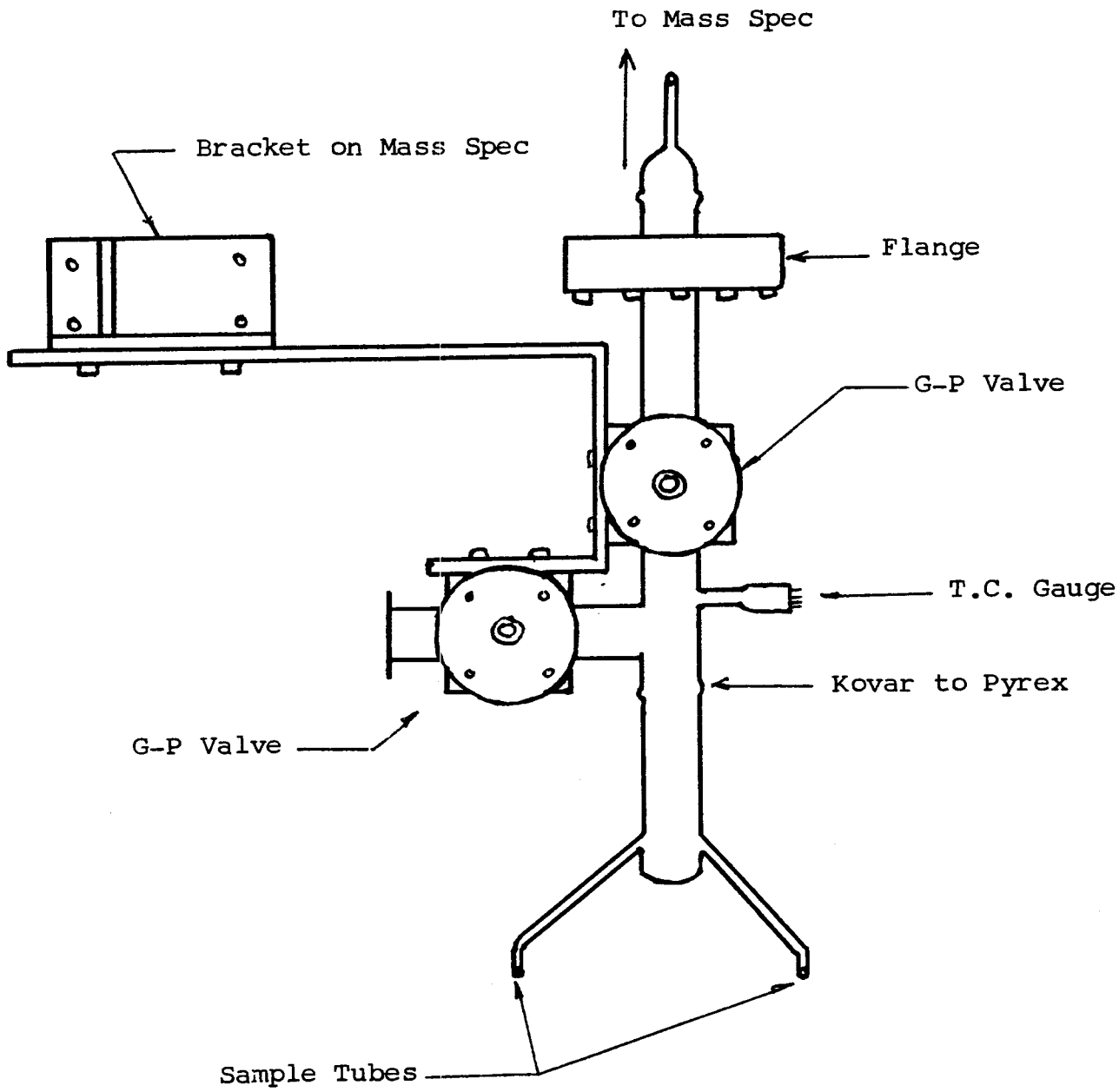

Figure 18

SCHEMATIC (TOP VIEW) OF THE PHOTOLYSIS TRAIN

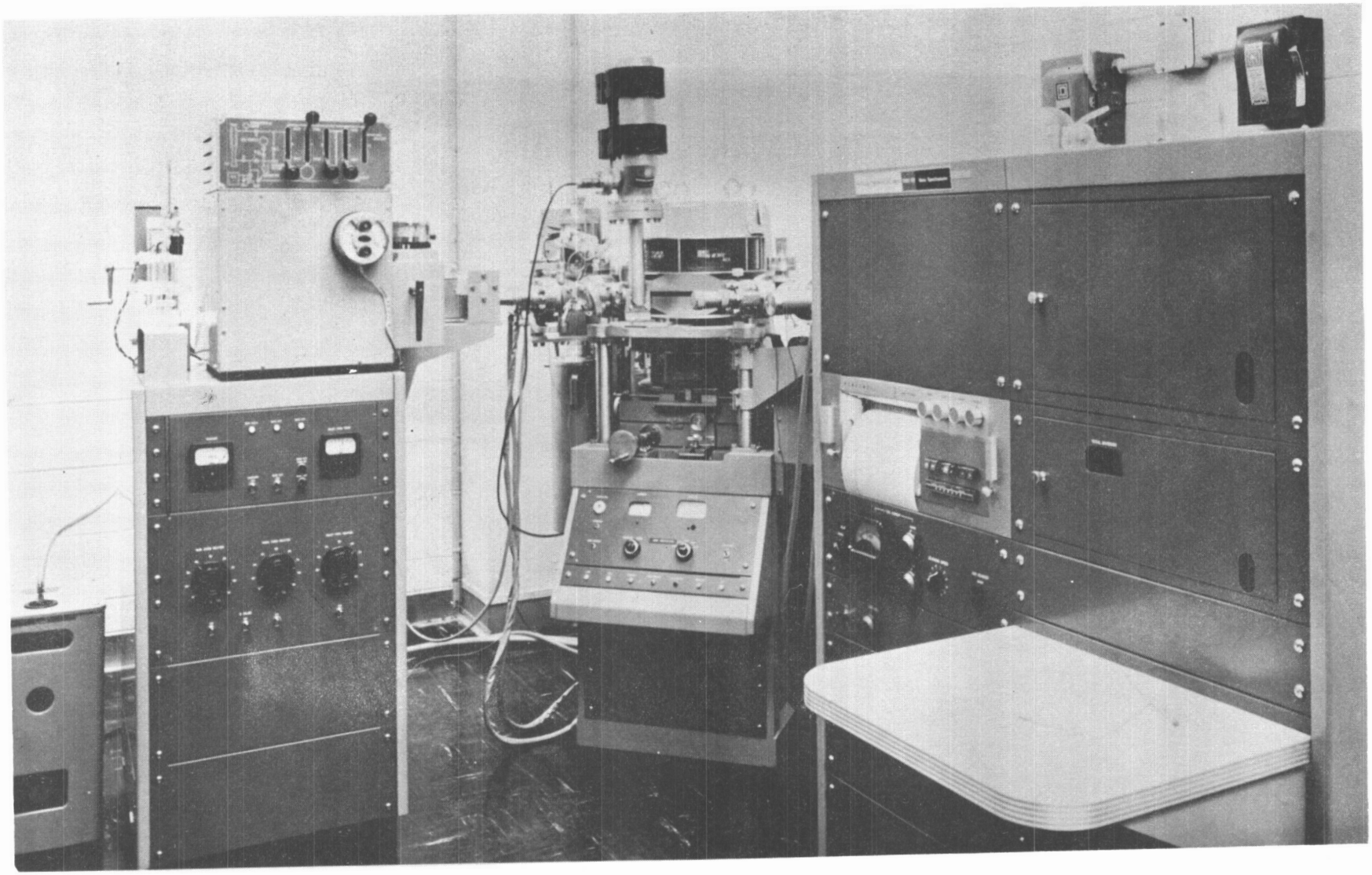

Figure 19

THE HITACHI RMU-6D MASS SPECTROMETER

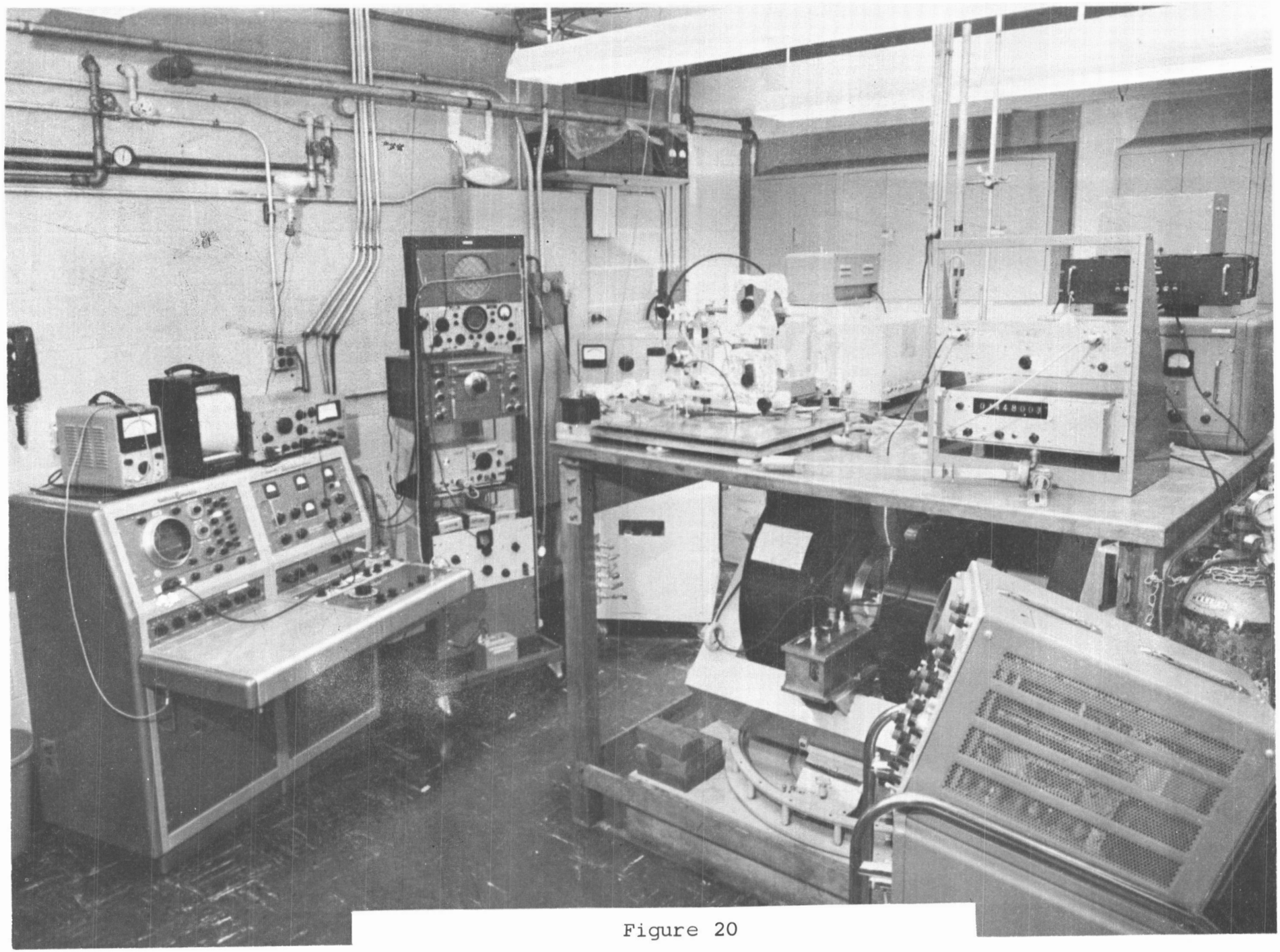

Figure 20

THE ELECTRON-SPIN-RESONANCE SPECTROMETER

A mass spectrum was obtained while pumping and while the sample was held at room temperature. Masses out to 625 to 630 were noted in the spectrum. Peaks at every mass were visible out to 250 mass units. Beyond 250 m/e, distinct groups of peaks were noted whose corresponding major peaks repeated every 14 and 16 mass units. This uniform repetition is due to successive losses of $-CH_2-$, -O- and -Si- with respective masses of 14, 16 and 28. The presence of mass 31 indicates a CH_3O^+ ion present either initially in the sample or formed by rearrangement in the ion source. A reasonably intense peak at m/e = 15 indicates CH_3^+ fragments from polymer. Other than these observations, the spectrum is complex and shows a relatively small amount of hydrocarbon peaks.

The sample was then cooled with liquid nitrogen and ultraviolet irradiation of the sample was initiated. Attempts to obtain mass spectra after 20 minutes and 1 hour after start of irradiation failed because of instrument malfunction. The sample was still at -192°C for these attempts.

Pumping on the samples was interrupted by closing the valve to the mass spectrometer and irradiation continued for another 1-1/2 hour while the sample was held at -192°C. At the end of the 2-1/2 hour irradiation period the ultraviolet lamp was turned off. An attempt was made to leak in whatever products had accumulated in the sample tubes. Although a pressure increase was observed when the valve was opened and the sample was at -192°C no spectra was obtained again because of instrument malfunction.

At this time, the instrument difficulty was corrected but in the meantime the sample was allowed to warm up to room temperature. While warming considerable bubbling was observed in the sample as it became more liquid. When the bubbling subsided, a mass spectrum was obtained; the sample was then at room temperature.

The mass spectrum obtained under these final conditions just mentioned was significantly different from the initial spectra where the sample was at room temperature before irradiation. Most significant was the lack of spectrum beyond approximately 350 mass units whereas peaks out to 625 to 630 were noted previously. This suggests removal of the higher molecular weight fragments by some means such as polymerization induced by the irradiation. The intensity of mass 31 was considerably increased along with masses at 27, 29, 41, 43, 45, 59 and 74 and a decrease of mass 73. The overall intensity of the final mass spectrum peaks increased, but the increases or decreases were disproportionately magnified. Some of the peaks (m/e = 27, 29, 41, 43) indicate saturated hydrocarbons with 2 and 3 carbons. The changes in m/e = 45, 59 and 74 could indicate an increase in the quantity of lower molecular weight Si molecules or increased branching in the polymer. The total spectra was again very complex and interpretation beyond that just discussed was not attempted.

At the completion of the period of irradiation one of the sample tubes was sealed off and, while still in liquid N_2, sent to the ESR laboratory. Mass spectra analysis was performed on the remaining sample.

The mass spectra data obtained on this sample should be rechecked because of the instrument malfunction and the ensuing changes in some of the control voltages, which obviates precise and unambiguous interpretation of the data. Although the data are thought to be reliable, the possibility of irregularities exists.

C. Analysis of ESR Spectra

The electron-spin-resonance absorption spectrum observed in the ultraviolet-irradiated silicone polymer LP-5 is essentially the same as those observed by other investigators (ref. 13,14). Trace recordings of the spectrum are shown in Figures 21 and 22, where Figure 22 is the same as Figure 21 multiplied in amplitude by a factor of five. This spectrum is essentially the same as

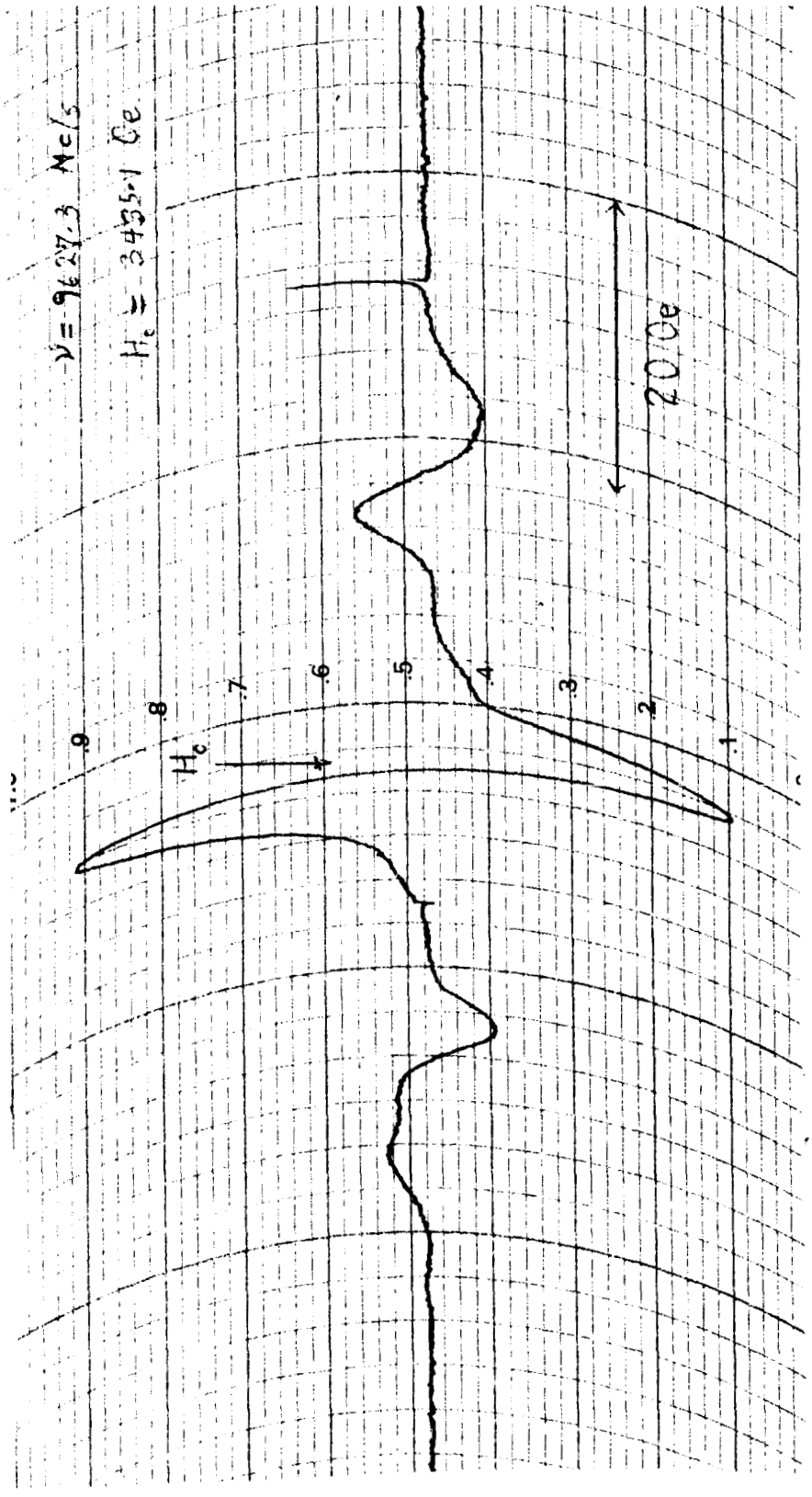

Figure 21

ELECTRON-SPIN-RESONANCE-ABSORPTION SPECTRUM OF LP-5 POLYDIMETHYLSILOXANE IRRADIATED WITH UV AT 77°K

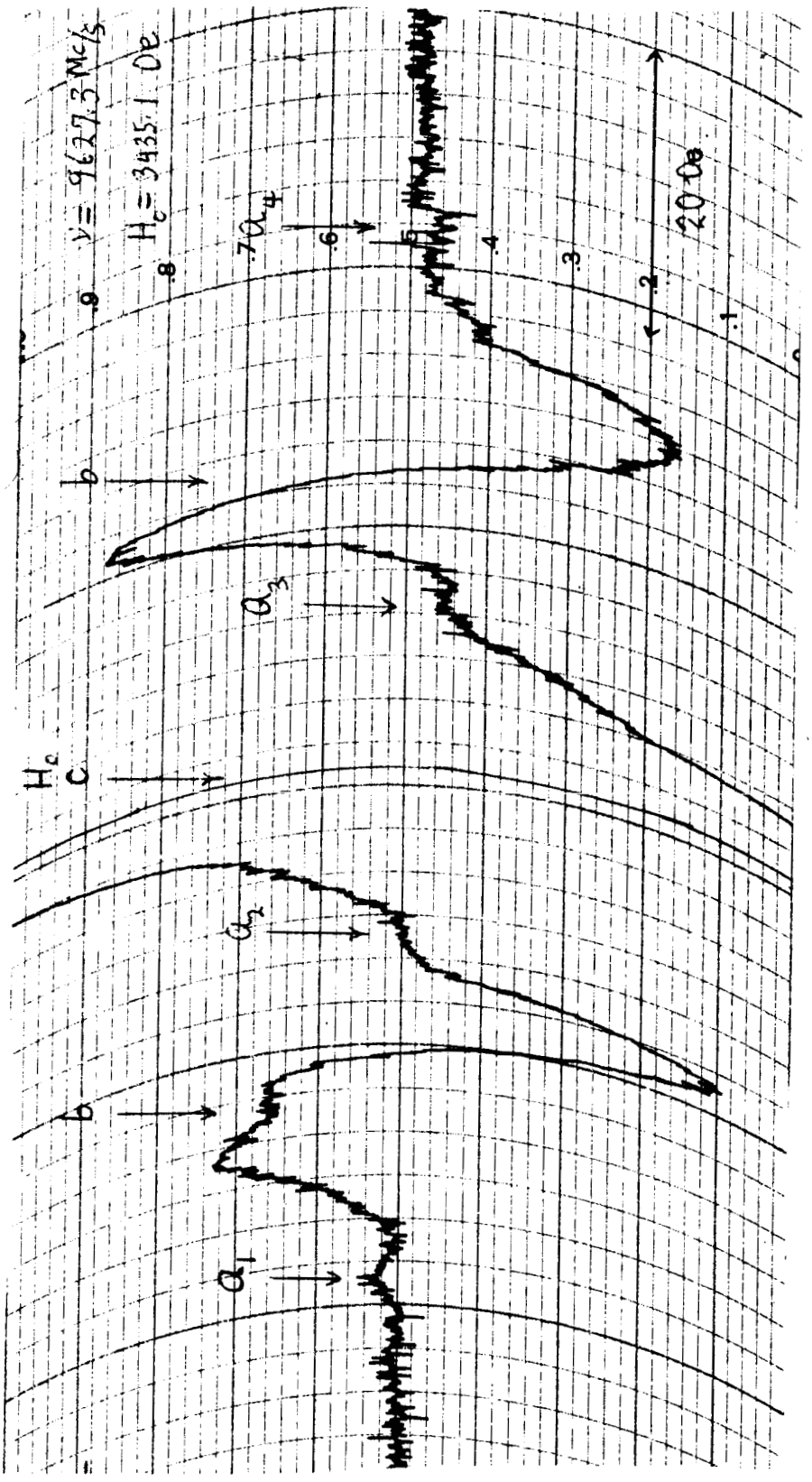

Figure 22

ELECTRON-SPIN-RESONANCE-ABSORPTION SPECTRUM OF LP-5 POLYDIMETHYLSILOXANE IRRADIATED WITH UV AT 77°K (Same as Figure 21 with Gain Times 5)

that observed in this laboratory on the irradiated, solid, cross-linked polydimethylsiloxane (ref. 15). Note in Figure 22, the weakest lines labeled a_i. Although the lines a_2 and a_4 are observed in these traces, if they are postulated to exist so as to form a quartet spectrum, this group of lines may be identified with $\cdot CH_3$ radicals which are unstable at 77°K. This probably explains their low intensity since these spectra were taken several hours from the time of irradiation.

The unpaired electron of the methyl radical interacts with three hydrogen nuclei, each having a nuclear spin quantum number of 1/2. Four magnetic dipole transitions are expected for this system corresponding to the nuclear magnetic quantum numbers $m = 3/2, 1/2, -1/2, -3/2$. The $m = \pm 3/2$ transitions are the outer lines labeled a_1 and a_4 in Figure 22. The $m = \pm 1/2$ would be the lines labeled a_2 and a_3 and are predicted to be three times more intense than the $m = \pm 3/2$ transitions since there are more ways of adding up the individual magnetic quantum numbers of the three hydrogen nuclei to give $m = \pm 1/2$. Energy eigen values for this system in the strong field limit are given by (ref. 15,16)

$$E(M, m) = g\beta HM + AMm \qquad (1)$$

where β is the Bohr magneton, H is the external magnetic field, g is the gyromagnetic ratio, A is the hyperfine splitting constant, and where we have neglected the nuclear Zeeman interaction. Transitions labeled a_1 and a_4 correspond to the $m = 3/2 \longrightarrow 3/2$, $M = 1/2 \longrightarrow 1/2$ and $m = -3/2 \longrightarrow -3/2$, $M = -1/2 \rightarrow 1/2$ transitions where M is the electron magnetic quantum number having two possible values $\pm 1/2$. The condition for resonance of these transitions are obtained from Equation (1) using the selection rules $\Delta M = \pm 1$, $\Delta m = 0$ giving

$$E(1/2,\ 3/2) - E(-1/2,\ 3/2 = g\beta H_1 + \frac{3}{2}\ A \qquad (2)$$

$$E(1/2,-3/2) - E(-1/2,\ -3/2) = g\beta H_4 - \frac{3}{2}\ A \qquad (3)$$

where H, and H_4 are the resonance field positions of a_1 and a_4. Since these transitions occur at constant microwave frequency ν , we set Equations (2) and (3) equal to $h\nu$, divided by $g\beta$ and solve for **A** and g. The result is

$$\frac{A}{g\beta} = H_4 - H_1 \qquad (4)$$

$$g = \frac{2h\nu}{H_1 + H_4} \qquad (5)$$

From the experimental data we have H_1 = 3400.2 oe, H_4 = 3466.1 oe at ν = 9627.8 Mc/s. Substituting these values into Equations (4) and (5) gives $A/g\beta$ = (22.1 ± 0.5) oersteds and g = 2.0037 ± 0.0010. These results are in good agreement with the values $A/g\beta$ = (21.9 ± 0.2) oersteds, g = 2.0026 (1) and $A/g\beta$ = 22.9 oersteds, g = 2.00242 (8) for CH_3 radicals trapped in Zeolite and CH_4 matrices, respectively (ref. 15,16). The errors in the parameters for the present case are large since the spectral lines are weak and not completely resolved.

Although Tsvetkov et al (ref. 13) have given tentative assignments to the remaining spectra labeled b and c in Figures 21 and 22, it is not clear that these identifications are correct. For example, the lines which they call group b appear to be a superposition of at least two spectra whereas this point was previously overlooked (ref. 14). It is not obvious that lines labeled b belong to a triplet spectrum as suggested by Tsvetkov (ref. 13). It may be possible to preferentially bleach out some of the lines at various temperatures to determine if these

assignments are valid. The g-value measured for the central component labeled c in Figure 22 is given by $g = 2.0026 \pm 0.0005$.

V. THE IRIF

The IRIF, an acronym for "In Situ Reflectance/Irradiation Facility," is a multiple-sample ultraviolet-simulation facility possessing in situ hemispherical spectral-reflectance-measurement capabilities. The IRIF was designed on this project with NASA funds (Contract NAS8-5379) and constructed with IITRI funds.

The design was initiated because of the requirement for more definitive studies of the behavior of thermal-control materials in vacuum as measured by hemispherical spectral reflectance *in situ**. Recent studies by a number of workers, includ- extensive studies at IIT Research Institute, have shown that ing zinc oxide, for example, undergoes an easily bleachable (oxygen) degradation in the infrared which cannot be observed by the usual post-exposure reflectance measurements (ref.17).

Criteria for the design of the IRIF included the following: (1) capability of making hemispherical-spectral-reflectance measurements in vacuum without removing the samples from the vacuum chamber; (2) capability of irradiating several samples simultaneously; (3) provision for maintaining the samples at controlled temperatures between 77°K and 370°K during irradiation; (4) construction of a device which is easily attached (and detached) to the Beckman DK-2A spectroreflectometer; and (5) capability of adding at a later date a low-energy proton irradiation source that would be compatible with the system design. Because it was desirable to make "absolute" spectral measurements using an Edwards-type sphere, in which the specimen is located in the center of the sphere, a sixth requirement was the necessity for constructing a sample-transfer mechanism.

A schematic of the facility constructed is presented in Figure 23 and a section of the assembly drawing is shown in Figure 24. The integrating sphere is patterned after Edwards

---

*In Situ means, in reality, measured in position. In the context of this discussion, in situ is taken to mean measured "in vacuo" without removal to another environment.

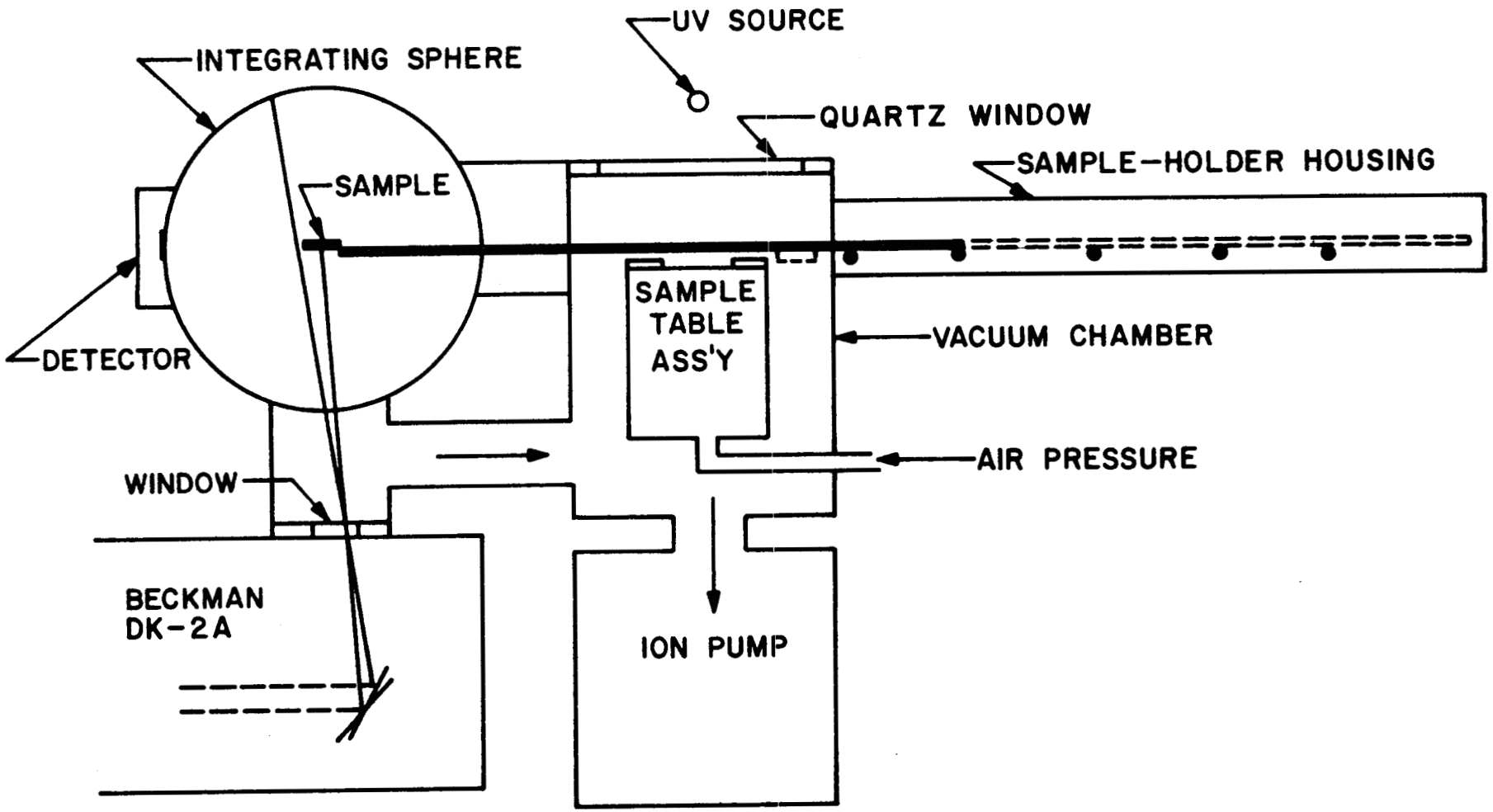

Figure 23

SCHEMATIC OF UV-IRRADIATION FACILITY WITH IN SITU REFLECTANCE CAPABILITY (THE IRIF)

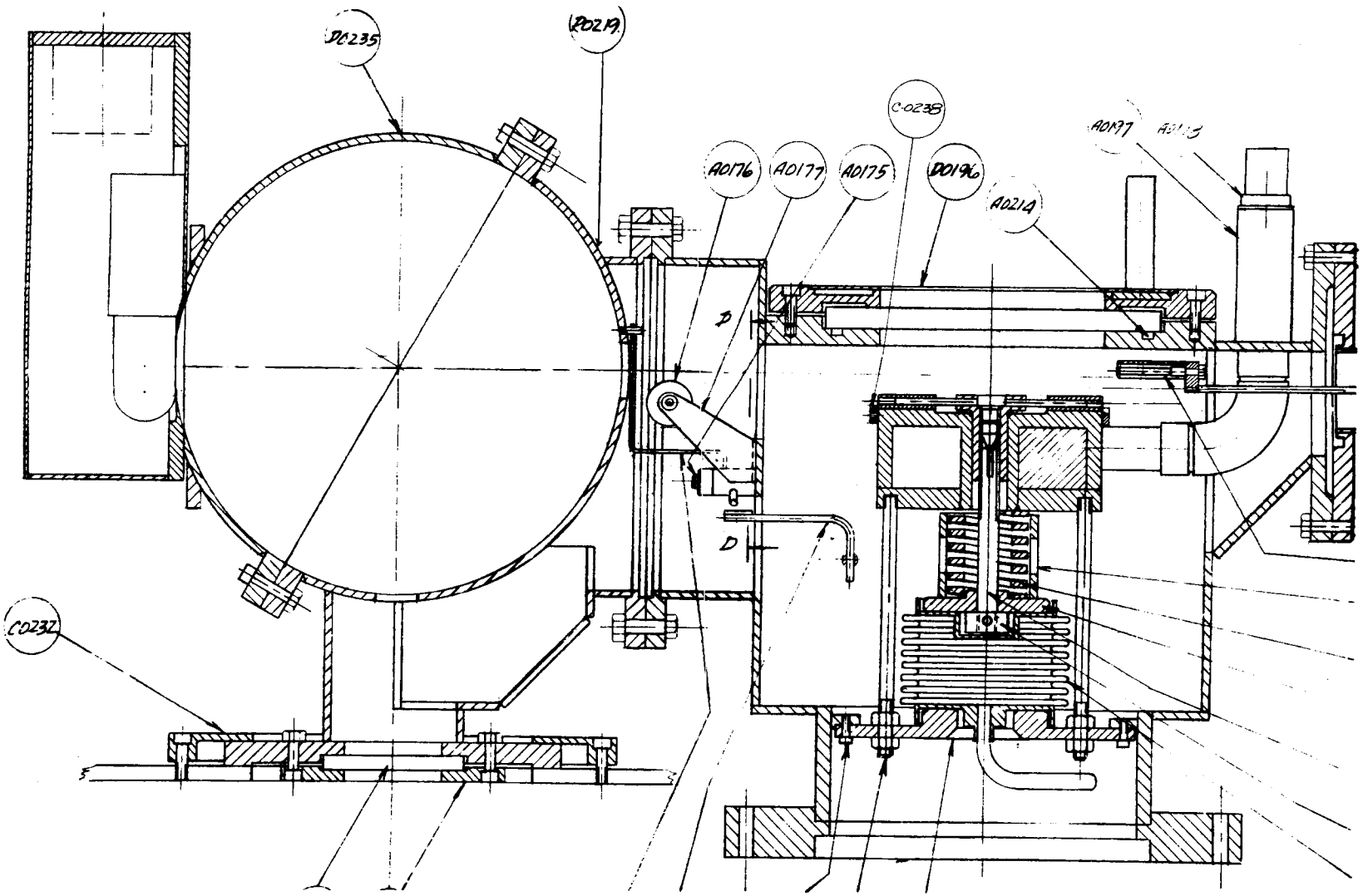

Figure 24

SECTION OF IRIF'S ENGINEERING ASSEMBLY DRAWING SHOWING INTEGRATING SPHERE AND UV-IRRADIATION CHAMBER

et al (ref. 18) modified for the Beckman DK-2A spectroreflectometer. The major features of the facility include: (1) operation of the integrating sphere in vacuum at $\sim 10^{-7}$ Torr by pumping through a manifold (through which the incident light beams pass) and through the shuttered sample aperture between the sphere and the vacuum chamber; (2) a 12-sample sample-interchange mechanism which maintains the specimens in contact with a temperature-controlled sample table ($\sim$ 77 to 370°K) and which permits the transfer of any one of the 12 samples to the integrating sphere for measurement and the subsequent return to the sample table for continued irradiation; (3) a dismounted Beckman DK-2A photo-multiplier tube sealed to the sample port and a dismounted DK-2A lead sulfide cell mounted to the inside wall of the evaucated integrating sphere; and (4) a quartz-irradiation-window-flange design which will permit the construction of a multiple-source housing above the sample table that contains both a low-energy proton source and an AH-6 lamp.

A schematic of the sample-table assembly and the sample-interchange mechanism is shown in Figure 25. The bottom drawing is a side view showing two cut-away samples in position; this view is also shown in Figure 24 as a detail from the assembly drawing. The samples are held by pins inserted into each. The pins are attached to a central, rotatable column. They are pressed to the liquid-cooled sample table by the spring mechanism shown in the drawings. The samples are released by pressurizing the bellows, which releases the pressure on the sample table by lifting the samples as shown. The entire sample-holding device can then be rotated by a bellows-equipped indexing arm; this arm is designated by the letter A in Figures 26 and 27, a top-view detail of the assembly drawing. A second bellows-equipped arm, designated by the letter B in Figures 26 and 27, moves the sample from the pin to the sample boat. The boat is subsquently transferred into the integrating sphere for measurement using a simple rack and pinion arrangement. The pinion is designated by the

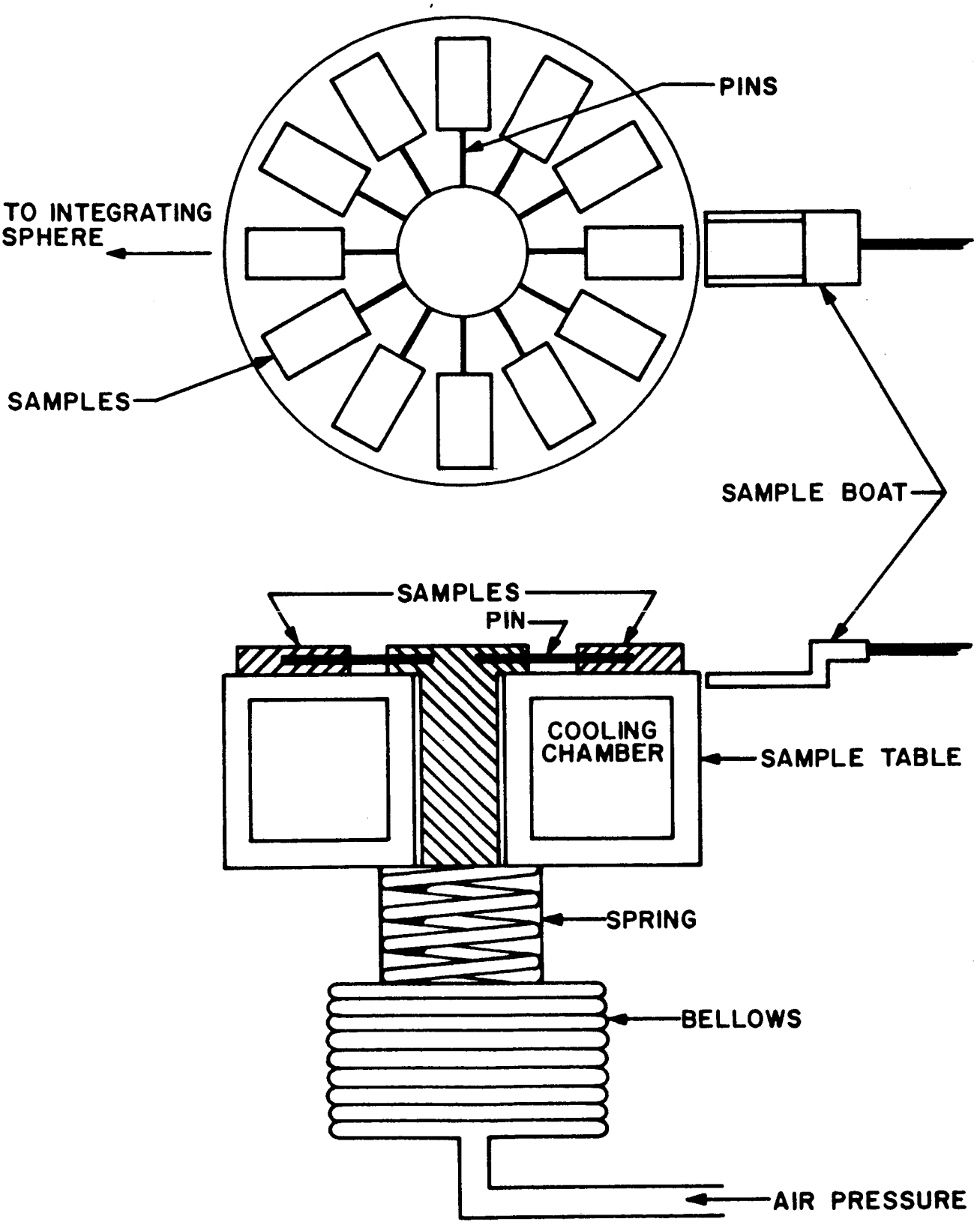

Figure 25

SCHEMATIC OF THE SAMPLE TABLE ASSEMBLY AND INTERCHANGE MECHANISM

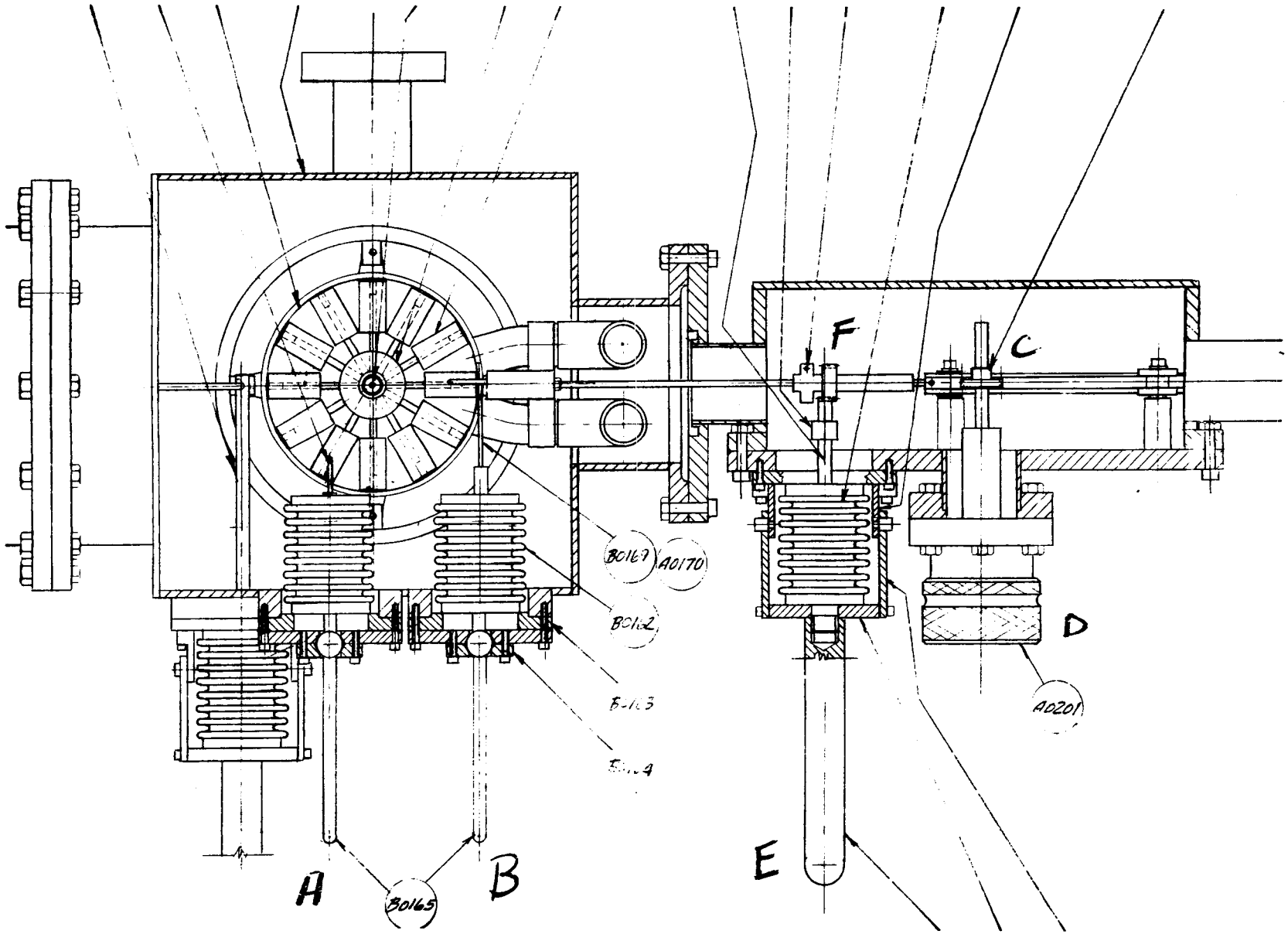

Figure 26

SECTION OF IRIF'S ENGINEERING ASSEMBLY DRAWING SHOWING
UV-IRRADIATION CHAMBER AND MANIPULATORS (TOP VIEW)

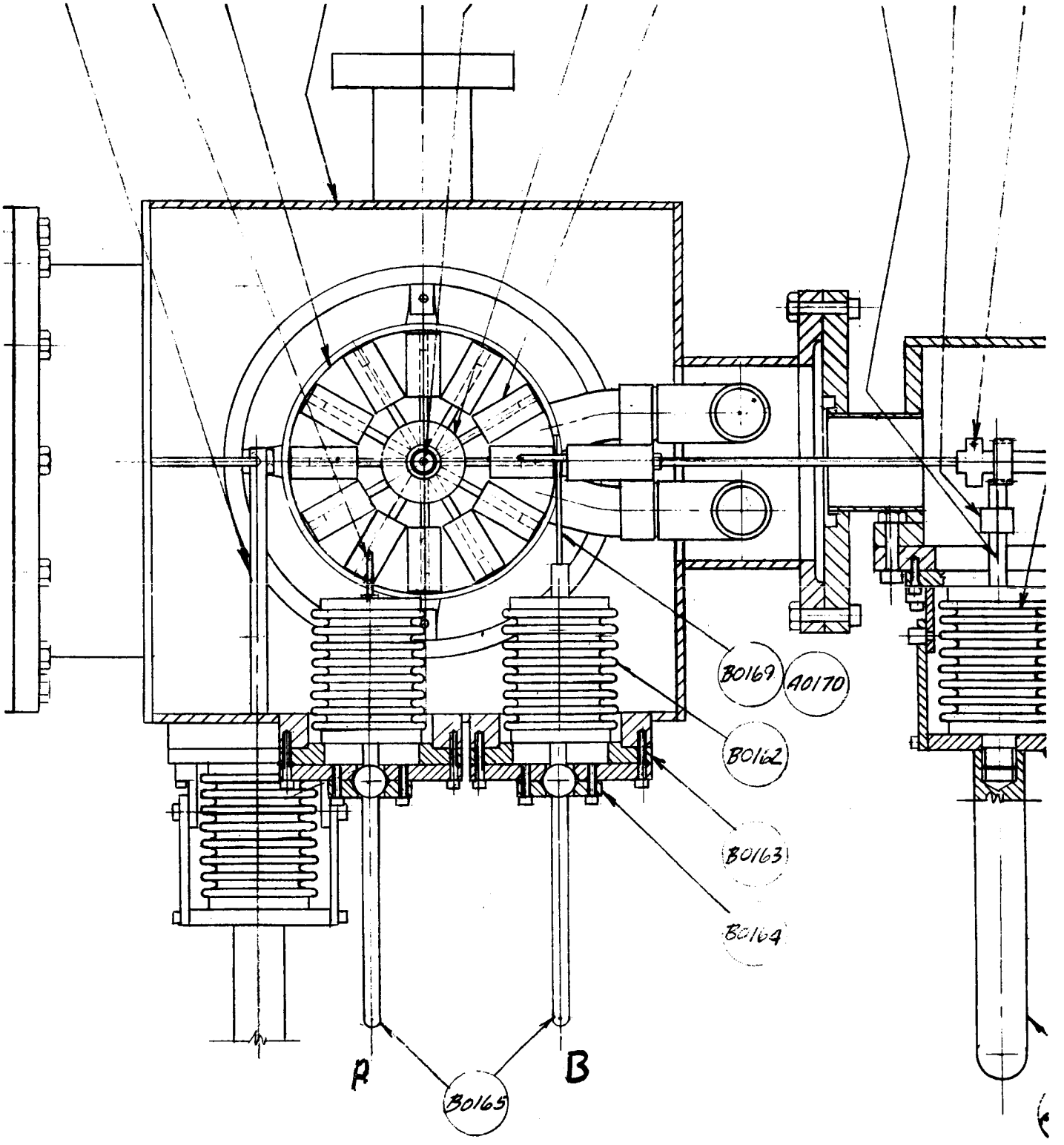

Figure 27

SECTION OF IRIF'S ENGINEERING ASSEMBLY DRAWING SHOWING THE UV-IRRADIATION CHAMBER (TOP VIEW)

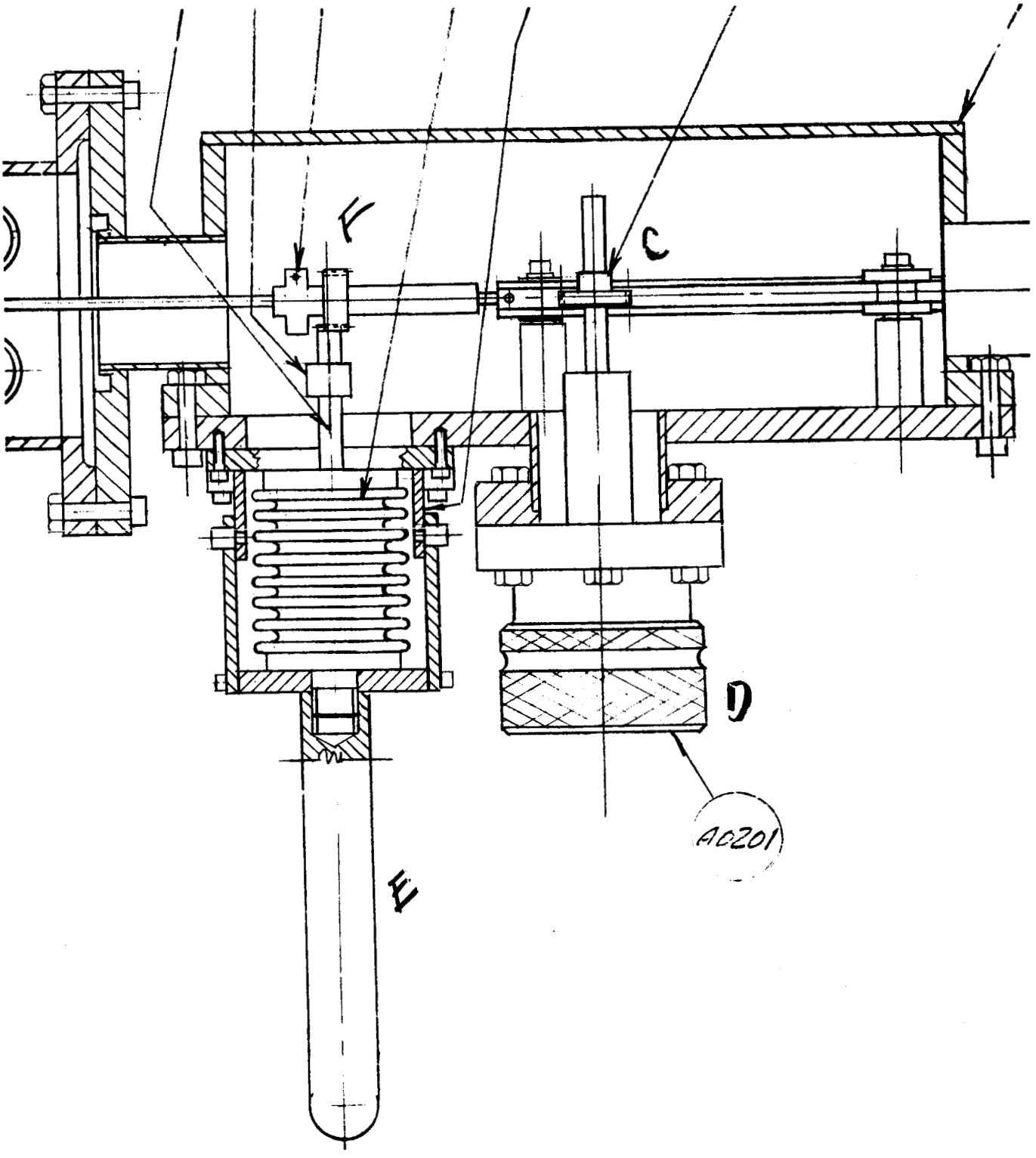

Figure 28

SECTION OF IRIF'S ENGINEERING ASSEMBLY DRAWING SHOWING MANIPULATORS, RACH AND PINION, AND MAGNETIC CHUCK

letter C in Figures 26 and 28; the gear is actuated by a magnetic chuck which is designated by the letter D in these same figures. The sample boat, with a sample in place, is turned 180° with a bellows-equipped manipulator prior to transfer into the integrating sphere. The manipulator is designated by the letter E in Figures 26 and 28 and affects the sample rotation with two gear segments (designated by the letter F).

Figure 29 shows the IRIF mated to the Beckman DK-2A spectrophotometer with the operator opening the shutter prior to transferring the sample into the integrating sphere. Figure 30 is a photograph of the 400 leter/sec Varian Vac Ion pump showing the chamber throat and the heavy-duty dolly. The entire facility is positioned by turning down the set-screw "stand-downs" into chocks permanently mounted to the floor. This procedure insures mating with the removable optical interchange which was constructed to replace the Beckman's "commercial" integrating sphere.

Figure 31 is a top view of the chamber showing the samples and sample-cooling table; the photograph also shows both the indexing arm and the sample-manipulator hook at approximately 12 and 9 o'clock, respectively. Figure 32 shows the permanently attached hemisphere of the integrating sphere with the sample holder (minus a sample) extended to the measurement position; the shutter is shown closed in this photograph.

The integrating sphere's removable hemisphere is presented in Figure 33. The IP28 photomultiplier tube is epoxied to a spherical segment which is in turn sealed to the integrating sphere with an indium gasket; the PM tube can be seen through the elliptical opening in the spherical segment. The lead sulfide cell with a 20 x 10 mm active surface, was obtained from Beckman and is mounted on the vacuum side of the spherical segment; the PbS-cell leads are soldered to copper leads that are located in fish spines epoxied into small holes drilled through the spherical segment as shown. The circuity for both the PM tube and the PhS cell are adapted from the Beckman facility and are mounted in the housing that is attached to the hemisphere.

Figure 29

THE IRIF MATED TO THE BECKMAN DK-2A SPECTROREFLECTOMETER

Figure 30

THE IRIF'S 400 LITER/SEC VAC-ION PUMP AND HEAVY-DUTY DOLLY

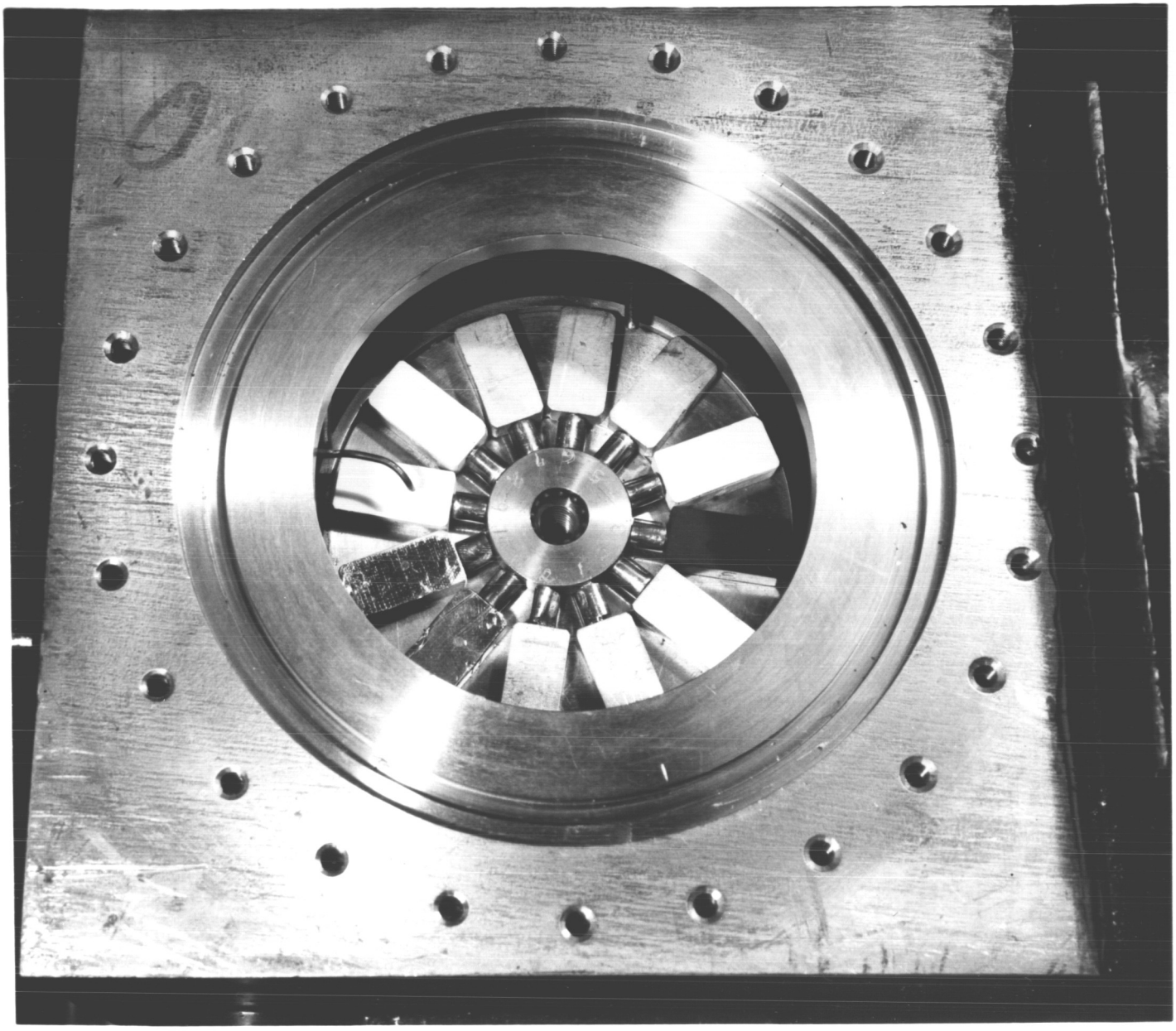

Figure 31

TOP VIEW OF THE IRIF'S UV-IRRADIATION CHAMBER SHOWING SAMPLES, SAMPLE TABLE AND MANIPULATOR ARMS

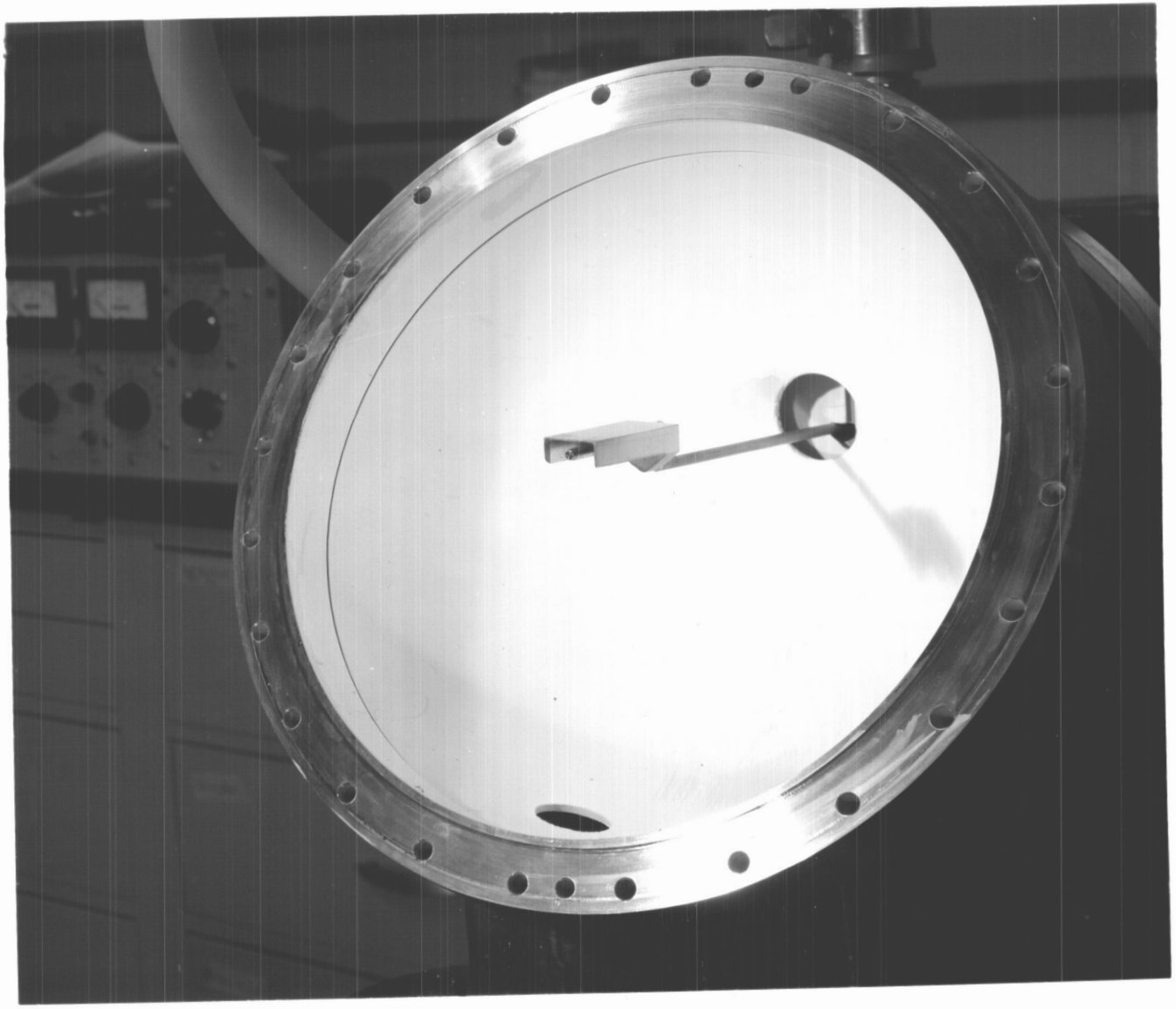

Figure 32

IRIF'S INTEGRATING-SPHERE HEMISPHERE SHOWING EMPTY SAMPLE HOLDER AND SHUTTER

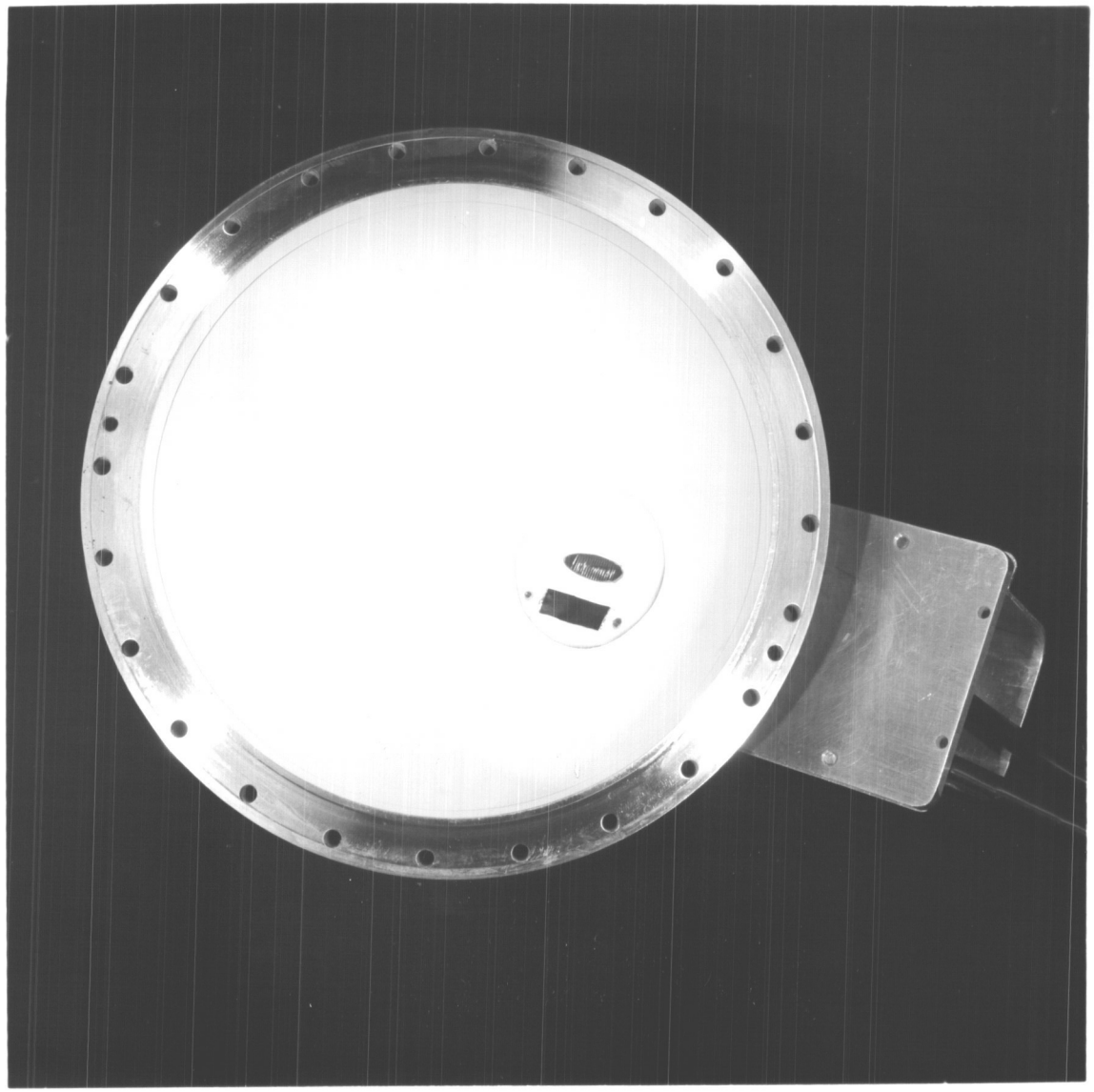

Figure 33

IRIF'S REMOVABLE HEMISPHERE SHOWING SPHERICAL SEGMENT WITH PHOTOMULTIPLIER TUBE AND LEAD SULFIDE CELL ATTACHED

Difficulties were encountered in vacuum checking the IRIF; the principal leaks were in the main-chamber and flange welds. These have been sealed and an initial pump-down of 5×10^{-6} torr was achieved in the MgO-smoked integrating sphere. The second pump down resulted in a vacuum of 2×10^{-7} torr in the main chamber.

Other difficulties which were encountered but which have been solved include: (1) construction and mounting of the dual-detector assembly on the sphere segment, (2) development of a suitable integrating-sphere coating, (3) incorrect geometry of the initial sample-manipulator hook and indexing rod (both actuated through bellows equipped levers), (4) weak construction of sample-manipulator hook and indexing rod, and (5) a poorly designed shutter-closing mechanism. In addition, a lever hold-down was required to prevent the sample-manipulator hook from depressing the rack (to which the sample boat is attached) when the sample is in the integrating sphere; depression of the rack throws the sample out of position and could eventually result in permanent deformation of the rack.

The integrating-sphere coating consists of a first coat of a zinc titanate-pigmented Owens-Illinois Type 650 resin paint followed by a light smoking (0.5 mm) with magnesium oxide. The zinc titanate paint possesses high ultraviolet reflectance down to wavelengths of 3400 A even without the MgO top coat.

The sample-manipulator hook and indexing rod were refabricated from stronger materials with a corrected geometry; the shutter-closing spring was replaced with a bar which closes the shutter when the actuator lever is moved in the opposite direction to that which opens it.

A more sturdy optical-interchange assembly must be designed and constructed. Although the assembly first constructed can be used with care, it can be easily knocked out of alignment. Also, the sample-holder rod will eventually have to be replaced with a stronger rod.

Should we construct another facility, a window would be placed in the top of the housing in which the pinion and gear-segment manipulators are mounted; this would facilitate mating the two gear segments which turn the sample through 180°. Finally, in addition to constructing several sub-assemblies from stronger material, we would re-design the sample manipulator assembly required to move the sample from the table to the boat and back.

The mechanical operation of the IRIF, though not simple, can be performed easily with a little training. Removal of a sample from the cooling table to the integrating sphere requires from 1 to 2 minutes. The spectral measurement itself requires no more time than with the standard comparison-type Beckman integrating sphere.

Current studies involve fatigue and vacuum degradation studies on a pair of 10-cm x 10-cm lead sulfide photocells (series dark resistance 1.5 megohms) that were mounted in series to replace the PbS cell obtained from Beckman (which was accidently shorted out). Should vacuum fatigue or degradation effects be significant, it will be necessary to mount the PbS cells outside the sphere behind a sapphire window. In this respect, Eastman Kodak will not, we are informed, accept orders for lead sulfide cells after December 31, 1966; the 20 x 20 mm cells supplied by Beckman have been purchased from Eastman. We have purchased two 10 cm x 10 cm cells from Infrared Industries, Inc. and will test them mounted in series. The pair now in use (unknown manufacturer) differ from the 20 cm x 10 cm cell furnished by Beckman only by the fact that the slits open at 2.5 rather than 2.7-μ wavelength.

Other studies contemplated for the immediate future include the generation of the following data: (1) a 100% line, (2) a curve showing the uniformity of sphere coating, (3) comparison spectra between the IRIF and our other Edwards-type sphere attachment for the Beckman (in air and in vacuum), and (4) data on irradiated specimens of SP500 zinc oxide, S-13G, silicate-

treated zinc oxide, and zinc titanates among others. The first "production" simulation test is planned for late in December. The General Electric AH-6 mercury-argon high-pressure quartz lamp will be used with the IRIF in simulation tests funded under this contract.

VI. SUMMARY OF RESULTS

The most important results and conclusions are summarized in the following paragraphs:

(1) The protected rutiles from Lexington Laboratories, Inc. though lacking in high reflectivity, were surprisingly stable to ultraviolet irradiation in vacuum. They possessed $\Delta\alpha$'s of only 0.014 and 0.025 after 2000 ESH of irradiation (as wet-sprayed powders).

(2) Cabot's "flame-process" rutile, A-54-2 zinc titanate, and the double zirconium silicates of calcium and zinc did not develope the oxygen-bleachable infrared degradation which characterizes zinc oxide pigment.

(3) Very white specimens of zinc orthotitanate, metatitanate and sesquititanate were prepared. The zinc orthotitanate was whiter than either the SP500 zinc oxide or the TiPure FF anatase titania from which it was produced. Although the orthotitanate powders contained excess zinc oxide which served to suppress their near-ultraviolet reflectance, its extraction by acetic acid resulted in a pigment of exceptional reflectance down to 3400 A wavelength and excellent stability to ultraviolet irradiation in vacuum. These studies have shown that 900°C is the minimum temperature required to produce a satisfactory pigment and that extraction of zinc oxide is also essential.

(4) Commercial zinc titanate (New Jersey Zinc's A-54-2) was used to prepare silicone paints based upon RTV-602 and Owens Illinois Type 650 glass resin. The elastomeric paint based on RTV-602 possessed one of the lowest solar absorptances which we have observed for a non-inorganic coating, namely 0.12. Its $\Delta\alpha$ of 0.025 for 2000 ESH of ultraviolet irradiation was also excellent. An Owens-Illinois paint, though it possessed a higher α of 0.18, exhibited a $\Delta\alpha$ of only 0.01 in 2000 ESH of ultraviolet irradiation in vacuum. The α of 0.18 was due to the thinness of the coating.

(5) It was found that the combination 85% toluene, 10% isopropanol and 5% n-butyl acetate provides the best solvent system for RTV-602-based paints. Also, it was found that the following solvent combination provides the best overall properties for coatings based on Owens-Illinois Type 650 resin: 50% 190p ethanol, 25% toluene, 13% cellosolve and 12% methyl isobutyl ketone.

(6) Though more experimental data are required, the results of mass spectrometry and electron-spin-resonance absorption spectrometry of the low molecular weight LP-5 polymethylsiloxane of 1.6 Me/Si indicate that the predominant reaction at 77°K is dimethylation.

(7) The IRIF, an acronym for "In Situ Reflectance/Irradiation Facility" has been completed and pump-downs to 2×10^{-7} Torr were achieved. It has been found to operate satisfactorily both from a mechanical and optical standpoint.

APPENDIX

The zinc oxide extraction and determination which we have used with zinc titanate-batches A-129 through A-133 is the method of Warning and Stone as found in Low's Technical Methods of Ore Analysis (ref. 19).

Enough pigment to contain an estimated content of zinc oxide of 1 to 2 grams is extracted with 50 ml of 10% acetic acid using an Erlenmeyer flask of 250 ml capacity and a "wrist action" shaker. The mixture is shaken for 16-24 hours. The extract is then rinsed into an open beaker with distilled water and 30 ml of a 20% solution of ammonium sodium hydrogen phosphate and 10 ml of 20% ammonium hydroxide are added. Ammonium hydroxide (20%) is then added dropwise until the solution is neutral to phenophthalein (pink end-point). The solution is next back titrated with 10% acetic acid; one ml of 10% acetic acid is then added to completely precipitate the zinc ammonium phosphate (a fine crystalline solid which rapidly settles to the bottom of the beaker). The precipitate is filtered, rinsed with hot distilled water, ignited and weighed as zinc pyrophosphate. The zinc oxide is calculated as

$$ZnO = \frac{Zn_2P_2O_7}{1.87}$$

REFERENCES

1. M. Lucien Levy, Compte Rendu, 105, 387-80, 1887

2. M. Lucien Levy, Compte Rendu, 107, 421-23, 1888

3. M. Lueien Levy, Ann. Chim. Phys., (6), 25, 433-59, 1892

4. L. Passerini, Ghaz. chim. ital., 60, (12), 957-62, 1930

5. N.W. Taylor, Z. Phys. Chem., B9 (4) 241-64, 1930

6. S. S. Cole and W. R. Nelson, J. Phys. Chem., 42 (2) 245-51, 1938

7. B. A. Loshkarev, Steklo i Keram, Vol 19, No. 3, 22-66, 1962

8. F. H. Dulin and D. E. Rase, J. Amer. Cer. Soc., 43, (3), 125-31, 1960

9. S. F. Bartram and R. A. Slepetys, J. Amer. Cer. Soc., 44, (10) 493-99, 1961

10. B. A. Loshkarev, Steklo i Keram 19, (10) 21-24, 1962

11. B. A. Loshkarev, Trans. Uralsk Polyt. Inst. Symp., 117, 1962

12. T. Kubo and M. Kato, et al, Kogyo Kagaku Zasshi, 66 (4), 403-7, 1963

13. Yu. D. Tsvetkov, Yu. N. Molin and V. V. Voevodskii, Vysokomol. Soedineniya 1, 1805 1959

14. M. G. Omerod and A. Charlesby, Polymer, 4, 459, 1963

15. C. K. Jen, S. N. Foner, E. L. Cochran and V. A. Bowers, Phys. Rev., 112, 1169, 1958.

16. R. A. Serway, G. A. Noble, A. O'Donnell and E. S. Freeman, J. Phys. Chem. to be published.

17. G. A. Zerlaut et al, Development of Space Stable Thermal Control Coatings, Report No. IITRI-U6002-36, (February 1966) and IITRI-U6002-42, (July 20, 1966), Contract NAS8-5379.

REFERENCES CONT.

18. D. K. Edwards, J. T. Gier, R. Nelson, and R. D. Roddick, J. Opt. Soc., American, 51, 1279, 1961

19. A. H. Low, Technical Methods of Ore Analysis, Wiley and Sons, New York, 1919

Copy No. ____

DISTRIBUTION LIST:

Copy No.	Recipient
1-10 + reproducible	Director (M-P&C-MPA) National Aeronautics & Space Administration George C. Marshall Space Flight Center Huntsville, Alabama
11-12	National Aeronautics & Space Administration George C. Marshall Space Flight Center Huntsville, Alabama Attention: Mr. D. W. Gates (R-RP-T)
13	IIT Research Institute Division U Files
14	IIT Research Institute Editors, J. I. Bregman, Mail Files
15	IIT Research Institute F. O. Rogers, Division U
16	IIT Research Institute G. A. Zerlaut, Division U
17	IIT Research Institute F. Iwatsuki, Division K
18	IIT Research Institute Y. Harada, Division G
19	IIT Research Institute M. Swartz, Division G
20	IIT Research Institute W. Courtney, Division K
21	IIT Research Institute R. G. Scholz, Division U